NEAMS fuels modeling for fast reactors: FY24 accomplishments and outlook for FY25

Presenters: Christopher (Topher) Matthews, Jacob Hirschhorn, and Yinbin Miao

U.S. DEPARTMENT of ENERGY | Office of Nuclear Energy

Nitride Fuels Modeling Overview

Presenter: Christopher (Topher) Matthews

Contributors: Anton Schneider, P.C. Simon, Michael Cooper,

Uranium Nitride: Recent Accomplishments

- Developed first-of-a-kind mechanistic model for UN fission gas release and swelling
  - Revived dislocation model in BISON
  - Adapted lower-length scale UN parameters
- Quantitatively capturing swelling behavior in UN
- Expanded assessment data base and high burnup extension forthcoming in FY25

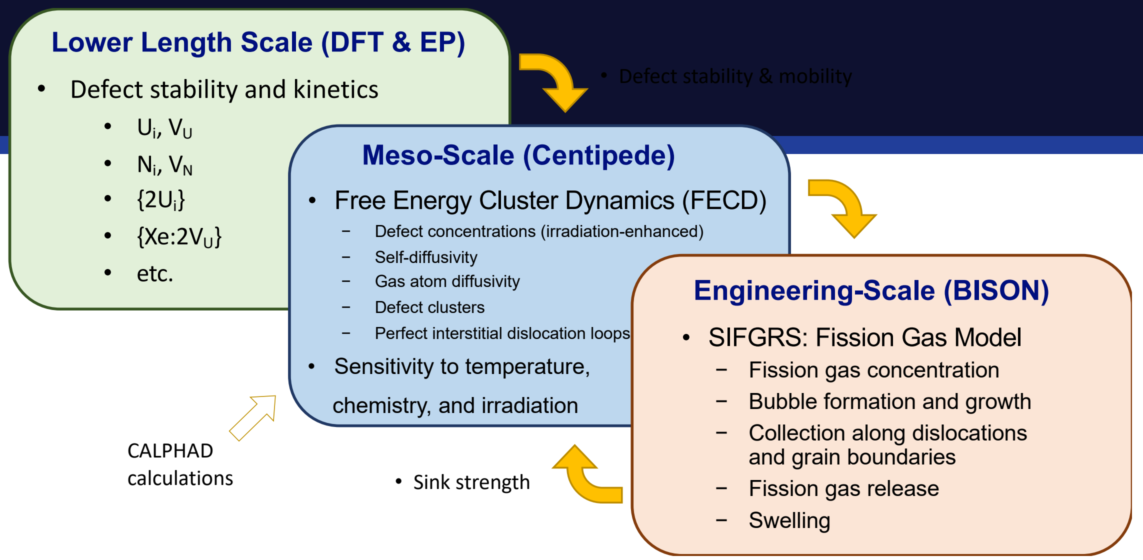

Uranium nitride capable BISON ready for external users

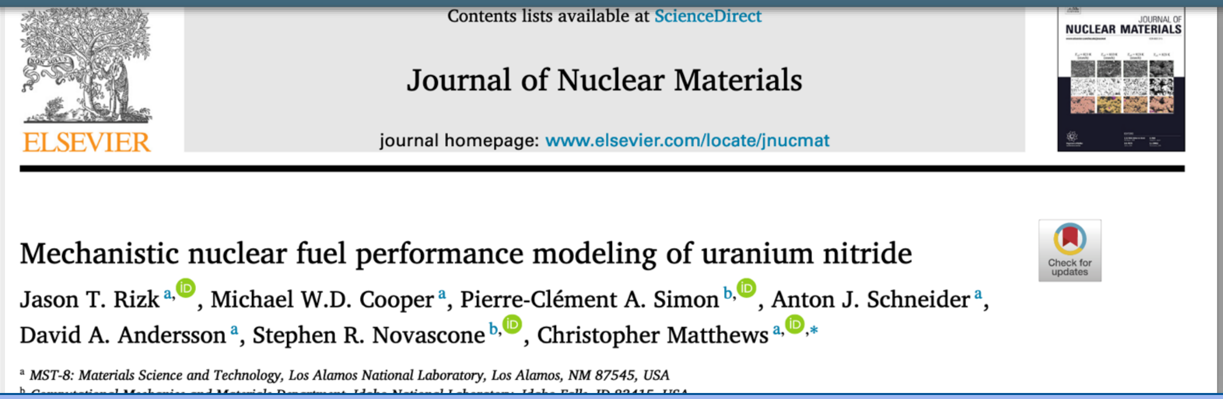

Contents lists available at ScienceDirect

Journal of Nuclear Materials

journal homepage: www.elsevier.com/locate/jnucmat

ELSEVIER

Mechanistic nuclear fuel performance modeling of uranium nitride

Jason T. Rizk [a], Michael W.D. Cooper [a], Pierre-Clément A. Simon [b], Anton J. Schneider [a], David A. Andersson [a], Stephen R. Novascone [b], Christopher Matthews [a,*]

[a] MST-8: Materials Science and Technology, Los Alamos National Laboratory, Los Alamos, NM 87545, USA

~3% FIMA

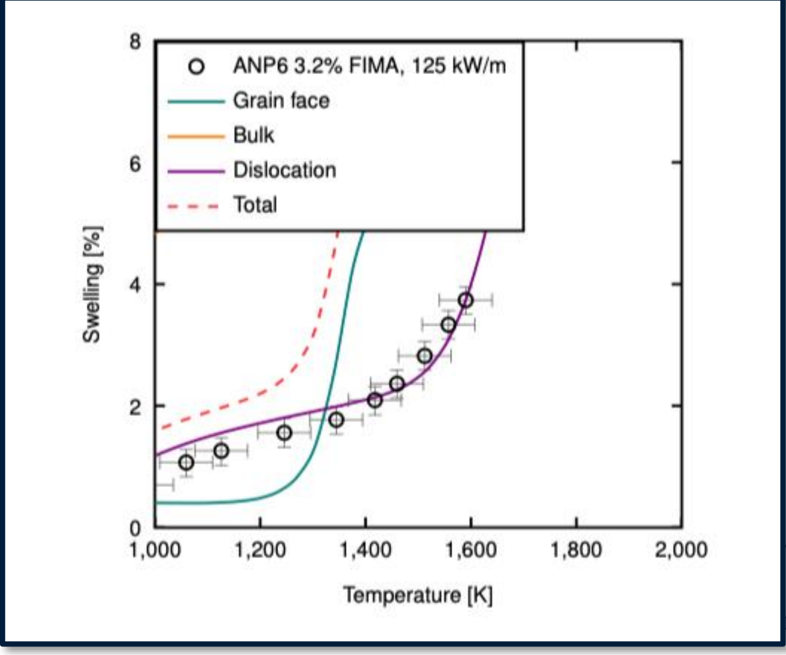

Continuing work focused on 1) chemistry dependence, 2) porosity dependence, and 3) application to TRISO

UN Modeling Approach: Capture breakaway swelling first

Mechanistic modeling allowed for mechanism not to be picked a priori

Experimental observation: "Breakaway Swelling"

- Sudden change in the rate that microscopic swelling increases with temperature once a threshold temperature is reached (Region $I \rightarrow II$)
- Greater burn-up causes lower transition temperatures

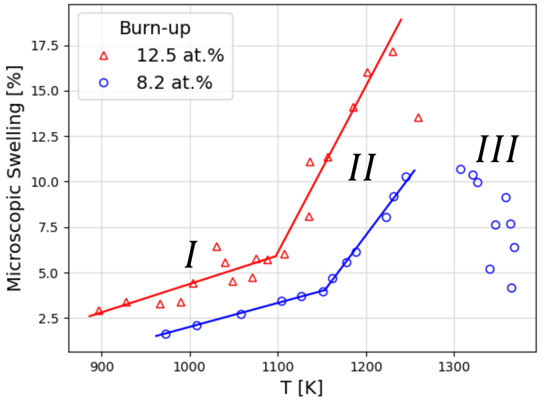

Microscopic swelling in MC

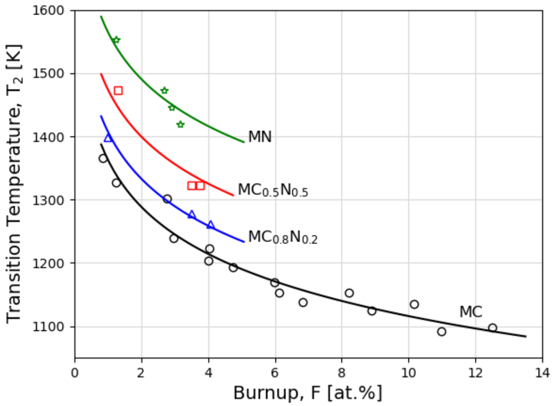

The transition temperature ($I \rightarrow II$) for breakaway swelling in MCN fuel

- Region II associated with both larger intra- and inter-granular bubbles
- Third region (III) of decreased swelling after a greater threshold temperature
  - Large interconnected grain boundary bubbles
  - Release of gas from grain interior into porosity

Need to understand this phenomenon for mechanistic fuel performance model

M. Colin, M. Coquerelle, I. L. F. Ray, C. Ronchi, C. T. Walker, H. Blank, *Nuclear Technology* 63, 442, 1983

Mechanism(s) responsible for the transition?

Extended defects consume point defects?

- The dislocation network more efficiently traps interstitials
- Vacancies trap at bubbles instead of annihilating through recombination

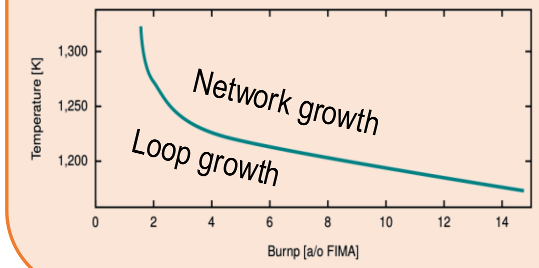

Calculated defect concentrations

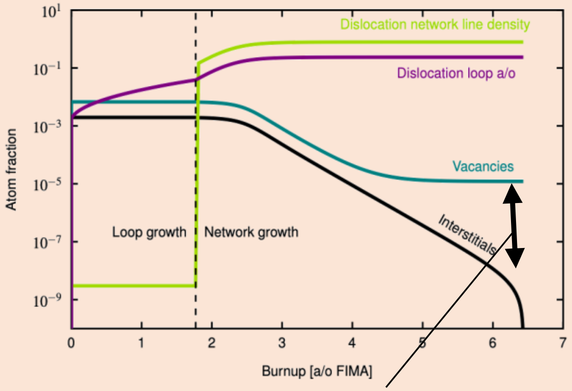

Increasing gap between point defect concentrations

Recrystallization?

- The accumulation of extended defects makes it energetically favorable to form new grain boundaries
- Grain boundaries trap gas atoms and grow larger bubbles

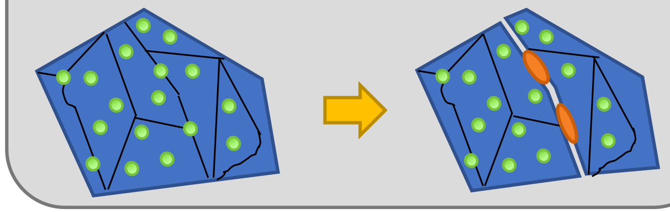

Diffusion mechanism transition?

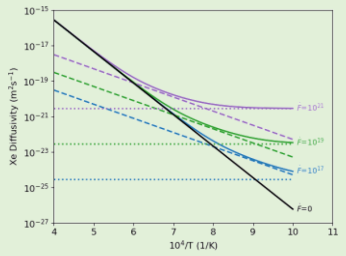

Modeling plan:
- Start with UO_2
- Adapt for UN

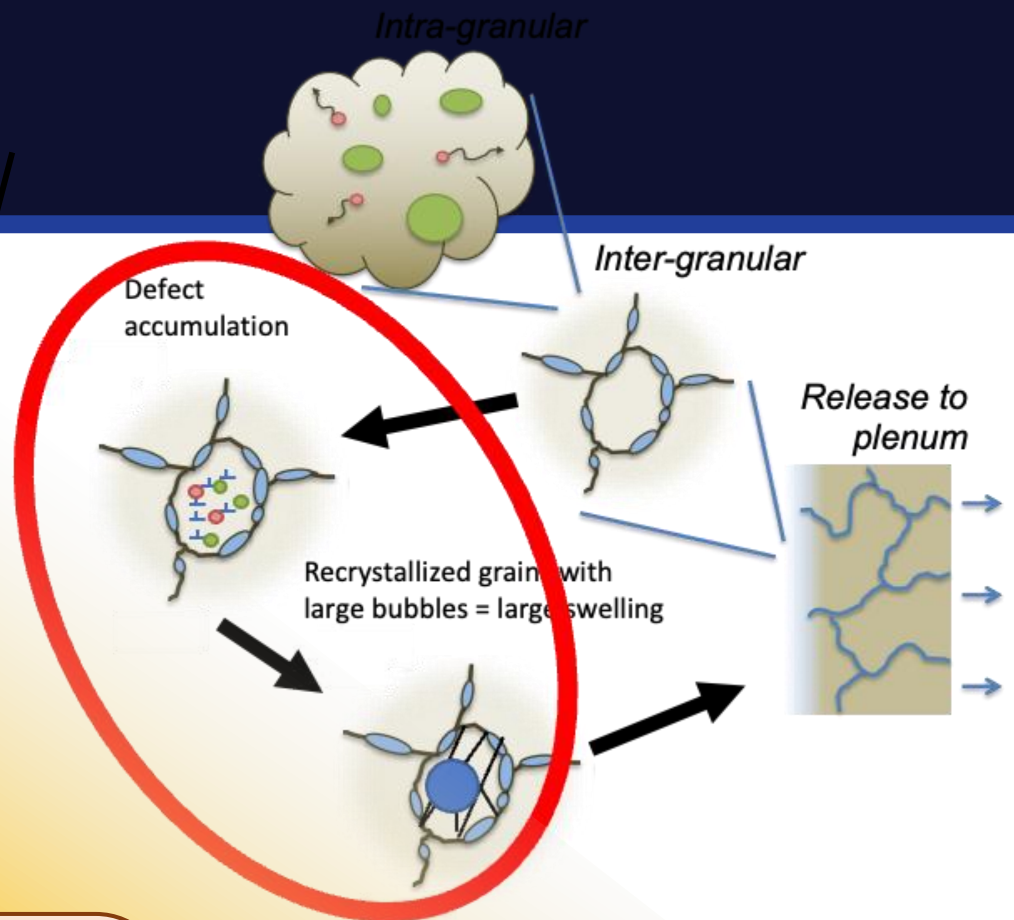

Lower Length Scale (DFT & EP)

- Defect stability and kinetics
  - U_i, V_U
  - N_i, V_N
  - $\{2U_i\}$
  - $\{Xe:2V_U\}$
  - etc.

- Defect stability & mobility

Meso-Scale (Centipede)

- Free Energy Cluster Dynamics (FECD)
  - Defect concentrations (irradiation-enhanced)
  - Self-diffusivity
  - Gas atom diffusivity
  - Defect clusters
  - Perfect interstitial dislocation loops
- Sensitivity to temperature, chemistry, and irradiation

CALPHAD calculations

- Sink strength

Engineering-Scale (BISON)

- SIFGRS: Fission Gas Model
  - Fission gas concentration
  - Bubble formation and growth
  - Collection along dislocations and grain boundaries
  - Fission gas release
  - Swelling

Mechanistic Model Results

- Quantitative Comparison to data with (almost) no calibration
- Upturn corresponds to self-diffusivity
- Constant dislocation density

~1% FIMA

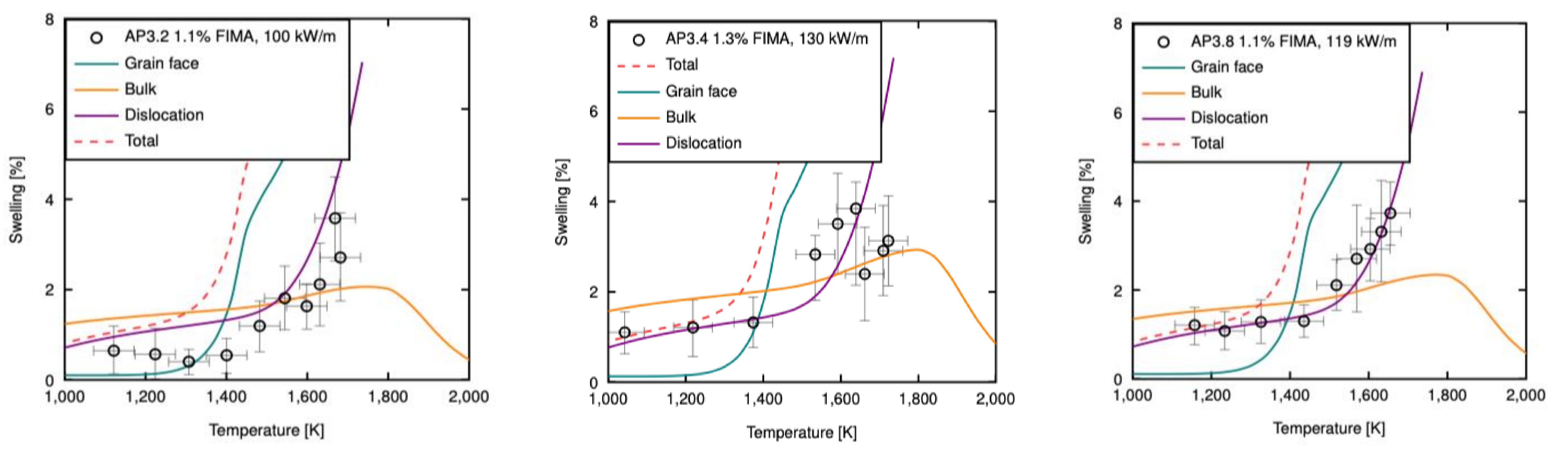

Mechanistic Model Results

- Quantitative Comparison to data with (almost) no c
- Upturn corresponds to self-diffusivity
- Constant dislocation density

Diffusivities

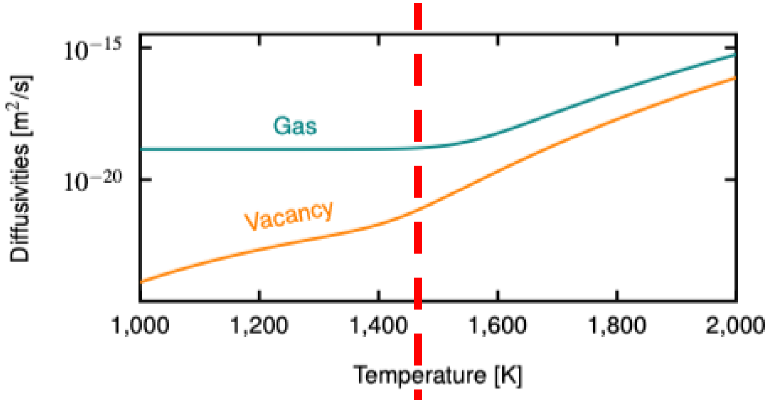

~1% FIMA

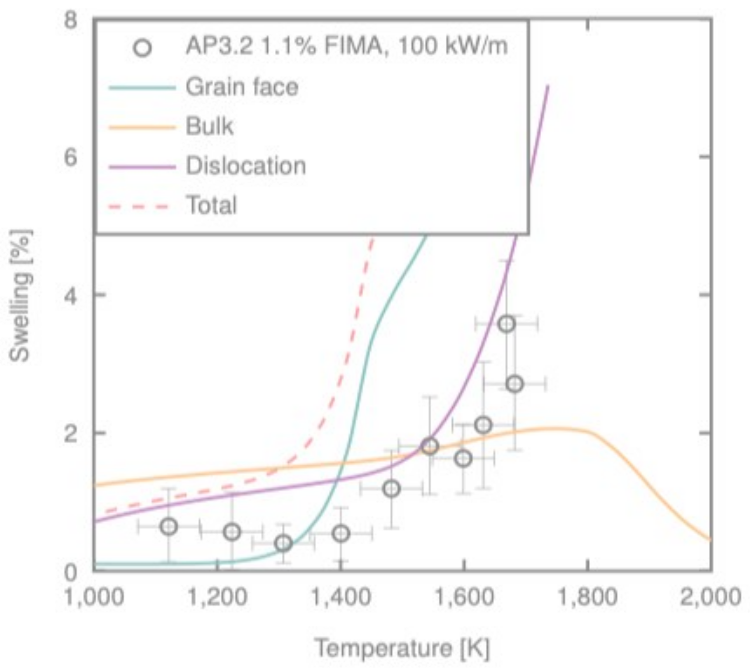

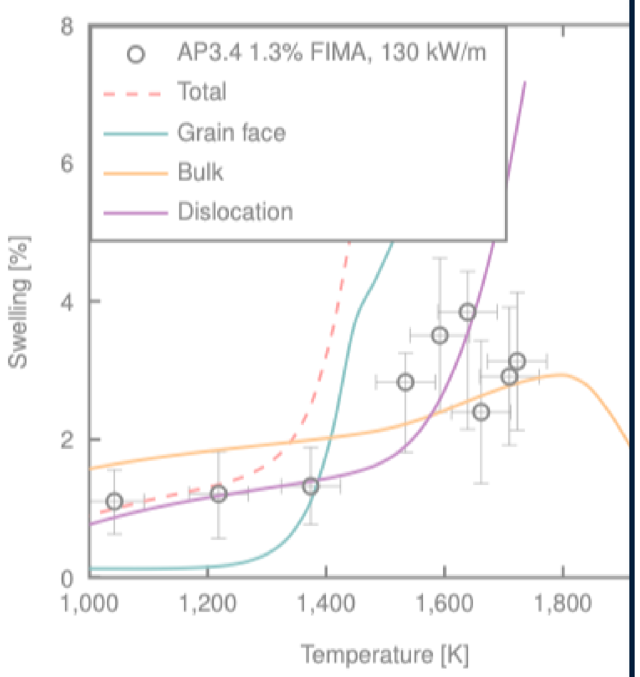

~3% FIMA

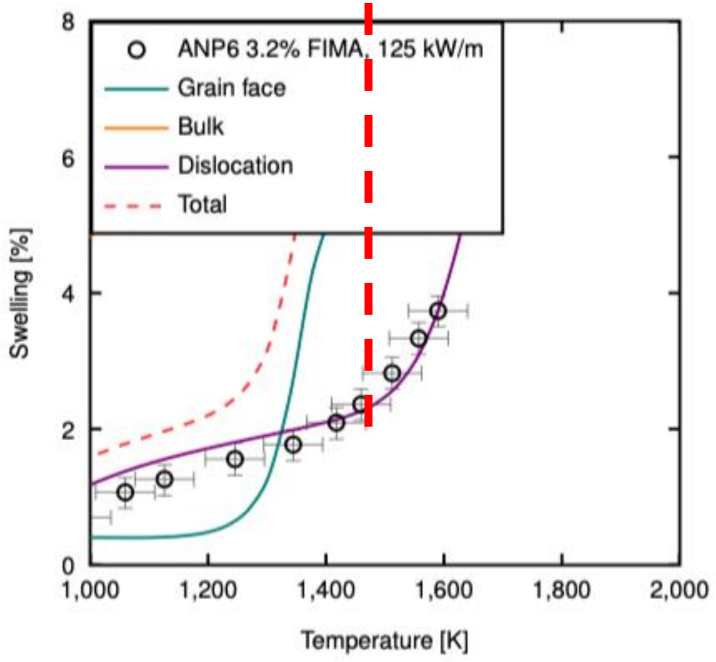

Integral experiments:
Combined assessments with same parameters

SNAP50-57-672 (MTR)

- Model with best historical data
- Temperatures [K]: 1430, 1500 (avg, max)
- Fsnrates [fsn/m³/s]: 1-1.5x10[19] (avg, max)

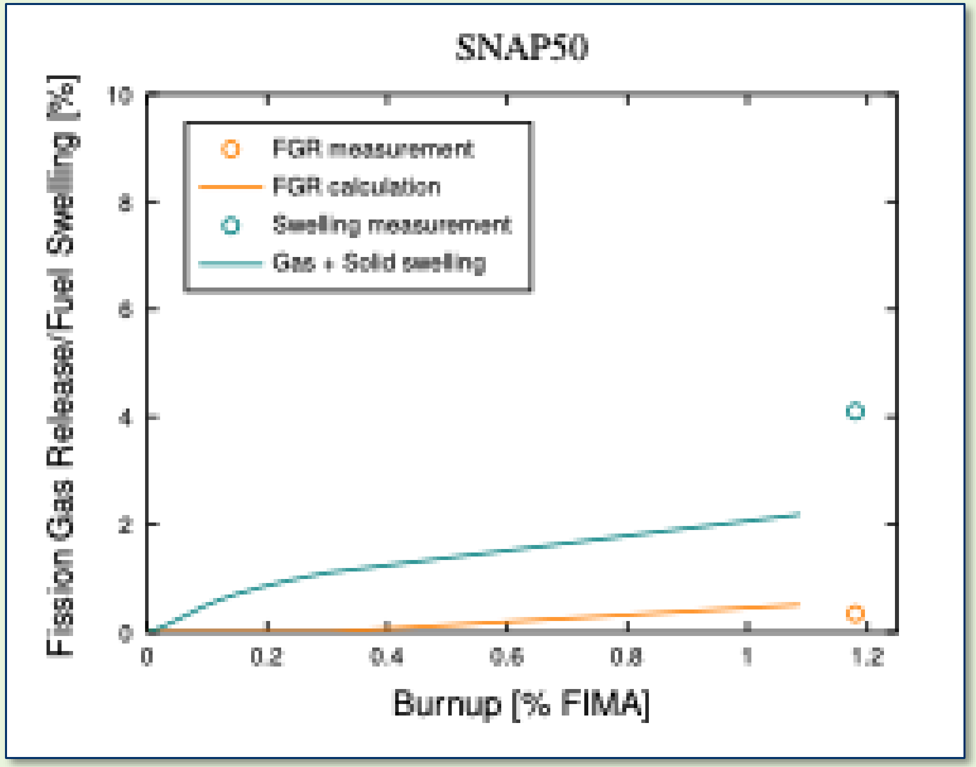

SP1 (EBR-II)

- Model with best historical data
- Temperatures [K]: 1800, 2050 (avg, max)
- Fsnrates [fsn/m³/s]: 3-3.3x10[19] (avg, max)

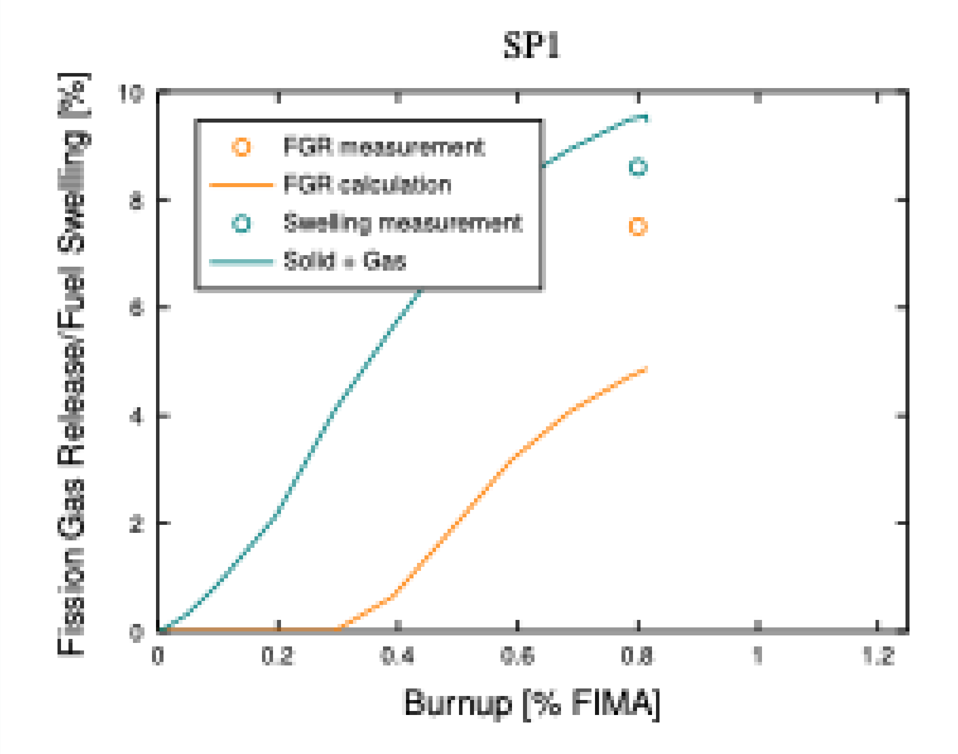

Uranium Nitride: Recent Accomplishments

- Developed first-of-a-kind mechanistic model for UN fission gas release and swelling
  - Revived dislocation model in BISON
  - Adapted lower-length scale UN parameters
- Quantitatively capturing swelling behavior in UN
- Expanded assessment data base and high burnup extension forthcoming in FY25

Uranium nitride capable BISON ready for external users

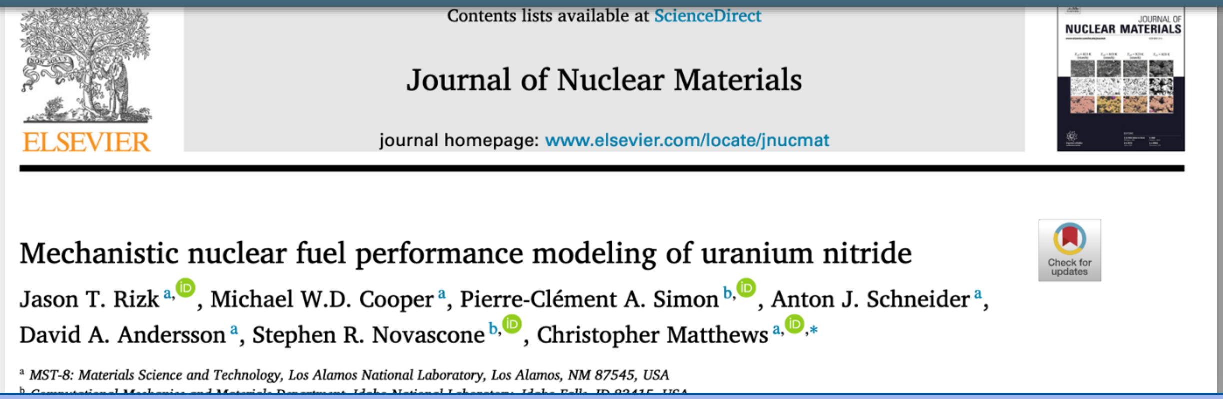
Contents lists available at ScienceDirect

ELSEVIER

Journal of Nuclear Materials

journal homepage: www.elsevier.com/locate/jnucmat

JOURNAL OF NUCLEAR MATERIALS

Check for updates

Mechanistic nuclear fuel performance modeling of uranium nitride

Jason T. Rizk[a], Michael W.D. Cooper[a], Pierre-Clément A. Simon[b], Anton J. Schneider[a], David A. Andersson[a], Stephen R. Novascone[b], Christopher Matthews[a,*]

[a] MST-8: Materials Science and Technology, Los Alamos National Laboratory, Los Alamos, NM 87545, USA

Continuing work focused on 1) chemistry dependence, 2) porosity dependence, and 3) application to TRISO

Lower Length Scale (DFT & EP)
- Defect stability and kinetics
  - U_i, V_U
  - N_i, V_N
  - $\{2U_i\}$
  - $\{Xe:2V_U\}$
  - etc.

- Defect stability & mobility

Meso-Scale (Centipede)
- Free Energy Cluster Dynamics (FECD)
  - Defect concentrations (irradiation-enhanced)
  - Self-diffusivity
  - Gas atom diffusivity
  - Defect clusters
  - Perfect interstitial dislocation loops
- Sensitivity to temperature, chemistry, and irradiation

CALPHAD calculations

- Sink strength

Engineering-Scale (BISON)
- SIFGRS: Fission Gas Model
  - Fission gas concentration
  - Bubble formation and growth
  - Collection along dislocations and grain boundaries
  - Fission gas release
  - Swelling

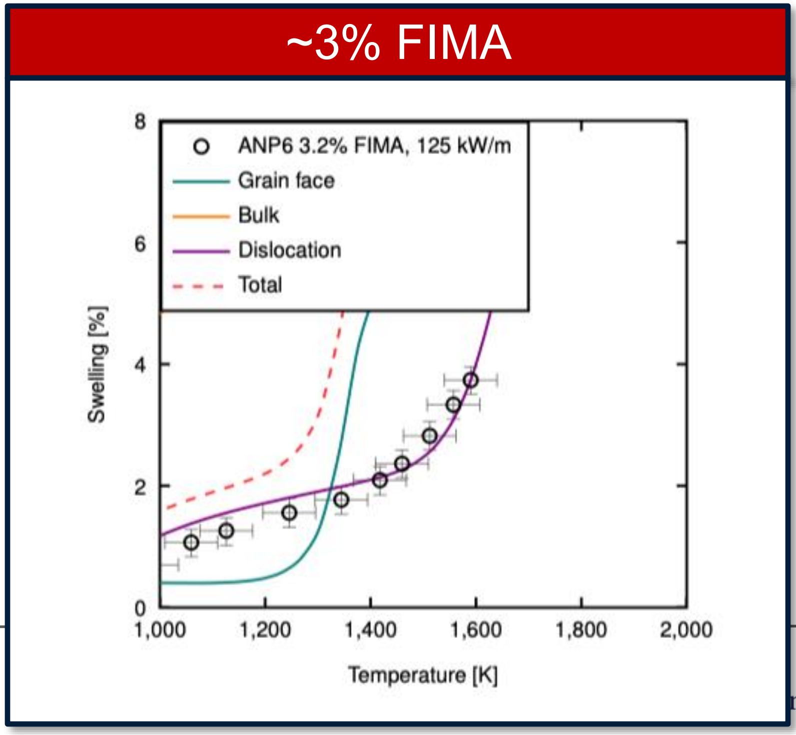

Metallic Fuels Capabilities Overview

Presenter: Christopher (Topher) Matthews

Contributors: Michael Cooper, Anton Schneider, P.C. Simon, Jacob Hirschhorn, Larry Aagesen, Yinbin Miao, Latif Yacout

Metallic fuel Highlights (1/2)

FCCI

- FY24: Developed mechanistic model for FCCI in U-Zr fuel
- Performed multi-scale calculations to determine effective lanthanide diffusivity
- BISON model for lanthanide production, transport, wastage layer growth
- Predictions agree well with X447, MFF-3
- Readily extensible to new fuel designs (annular, lined cladding)
- FY24: model for liquefaction risk on fuel side due to Fe diffusion from cladding to fuel

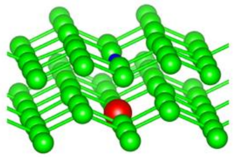

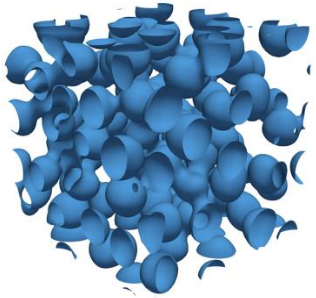

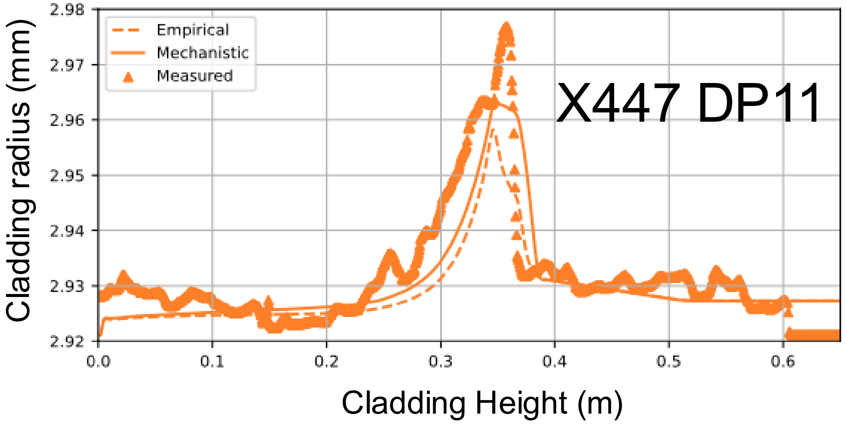

Baseline capabilities

- Metallic fuel baseline capabilities established
- Developed new correlations, models, physics
- VTB example forthcoming

Contents lists available at ScienceDirect

Journal of Nuclear Materials

journal homepage: www.elsevier.com/locate/jnucmat

ELSEVIER

Development and formulation of physics based metallic fuel models and comparison to integral irradiation data

Christopher Matthews[a,*], Stephen Novascone[d], Al Casagranda[c], Larry Aagesen[d], Cetin Unal[b], David Andersson[a]

[a] MST-8: Materials Science and Technology, Los Alamos National Laboratory, Los Alamos, NM 87545, USA
[b] W-13: Advanced Engineering Analysis, Los Alamos National Laboratory, Los Alamos, NM 87545, USA
[c] TerraPower LLC, 15800 Northup Way, Bellevue, WA 98008, USA
[d] Computational Mechanics and Materials, Idaho National Laboratory, Idaho Falls, ID 83415, USA

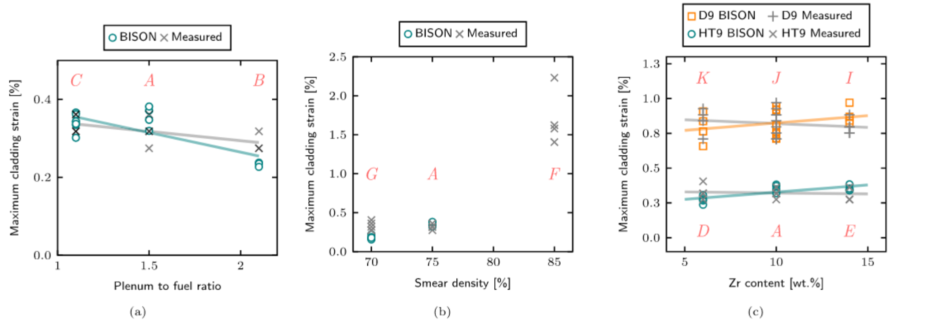

Fig. 9. Comparison between BISON results and EBR-II experimental data of cladding strain vs. a) plenum to fuel ratio with HT9 cladding, b) smear density with HT9 cladding, c) zirconium content [wt.%] with HT9 cladding, and d) zirconium content [wt.%] with D9 cladding.

Metallic fuel Highlights (2/2)
FIPD/OPTD Powered Metal Fuel Assessments

- **FIPD-BISON/OPTD-BISON Integration**
  - Data repository as a BISON submodule
- **Steady-State EBR-II Irradiation**
  - Established X423 Assessment
    - Focus: low-burnup fuel swelling
    - Powerful tools for swelling model V&V
  - Enhanced the Existing X447 Assessment
    - Focus: FCCI/cladding degradation
    - Advanced models adopted for improved predictions
- **Out-of-Pile Tests on EBR-II Irradiated Pins**
  - FBTA Assessment Case
    - 4 tests based on one fuel pin (X425/T418)
    - Improved empirical eutectic penetration correlations
  - WPF Assessment Case
    - 1 test (FM-1) based on one whole X425/T437 pin
    - Run till cladding breach at high temperature

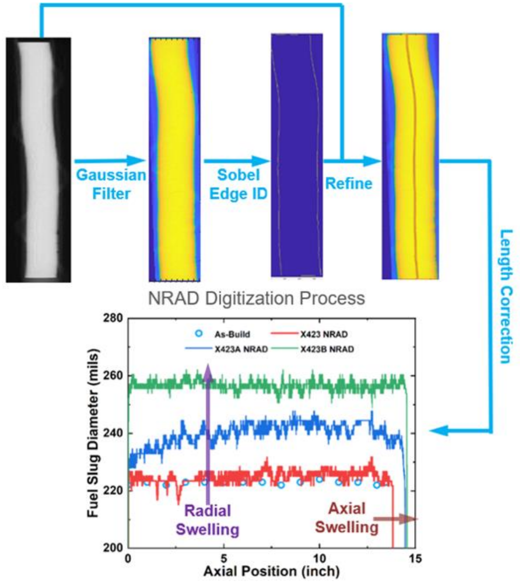

Use of NRAD data for swelling model assessment (X423)

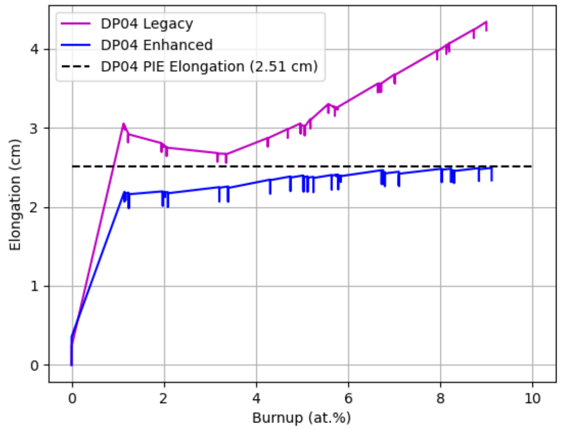

Improved fuel axial growth prediction (X447 enhancement)

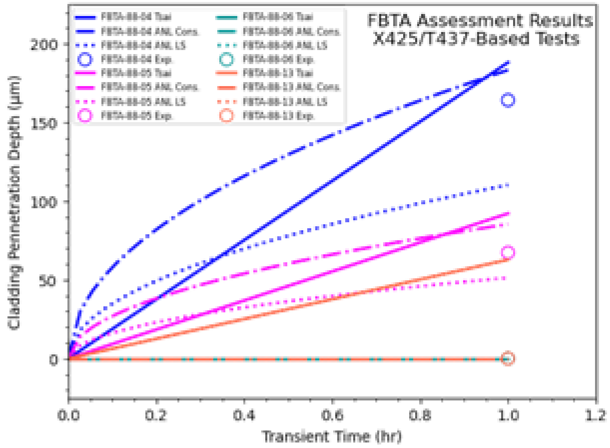

Cladding eutectic penetration kinetics (FBTA)

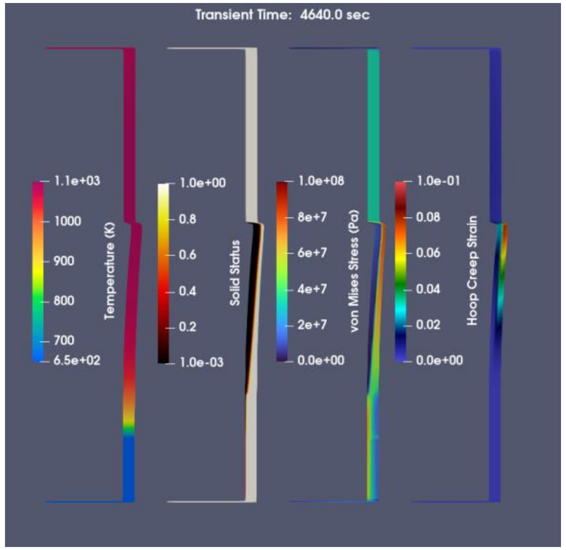

Transient cladding penetration & deformation (WPF FM-1)

FY2023 Publications

[1] Miao, Yinbin, et al. "BISON-FIPD integration enhanced low-burnup SFR metallic fuel swelling model evaluation framework." Nuclear Engineering & Design 414 (2023): 112611.
[2] Shu, Shipeng, et al. "Improved correlations of the fuel/cladding liquid penetration rate with the out-of-pile transient database." Nuclear Engineering & Design 417 (2024): 112819.
[3] Technical Report ANL-NEAMS-23/6
[4] Technical Report ANL-NEAMS-23/7

BISON Metallic Fuel Model Validation

Historical Database Implementation with FIPD & OPTD

Yinbin Miao, Aaron Oaks, Shipeng Shu, Abdellatif Yacout

Argonne National Laboratory

May 29, 2025

NEAMS Annual Review: Fast Reactor (Virtual)

[1] A.M. Yacout et al., *Nucl. Eng. Des.* 380 (2021) 111225
[2] A.M. Yacout et al., *Nucl. Technol.* 209 (2023) S109

BISON-FIPD Integration

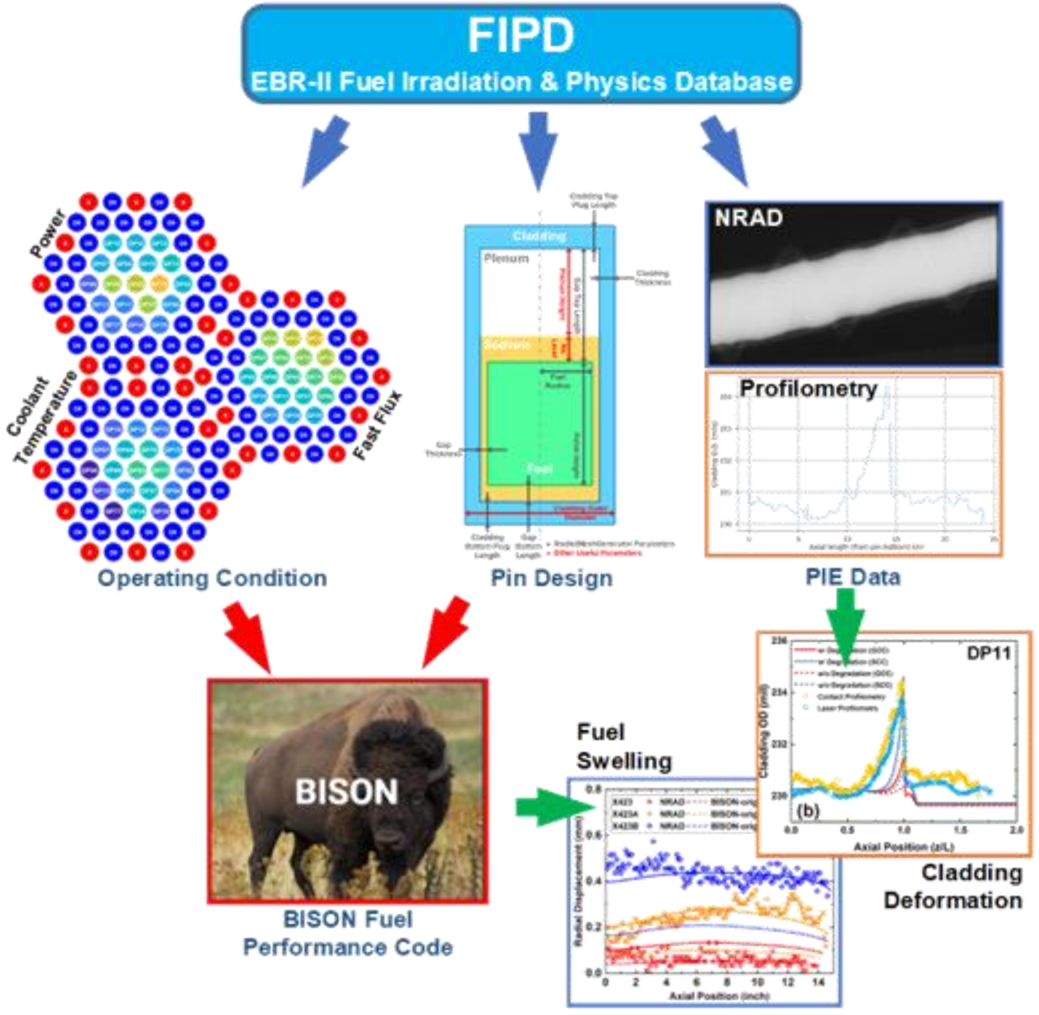

BISON-FIPD Integration Strategy

Verification & Validation

- **V&V BISON's Metal Fuel Capabilities**
  by Leveraging Legacy EBR-II Database w/ QA
  - FIPD†: steady-state in-pile irradiation experiments
  - Model implementation
    - Implement legacy descriptive fuel correlations.
    - Complement/validate adv. mechanistic models
  - BISON-FIPD integration tools to facilitate data usage
  - **BISON-FIPD Integration Powered Assessment Cases**

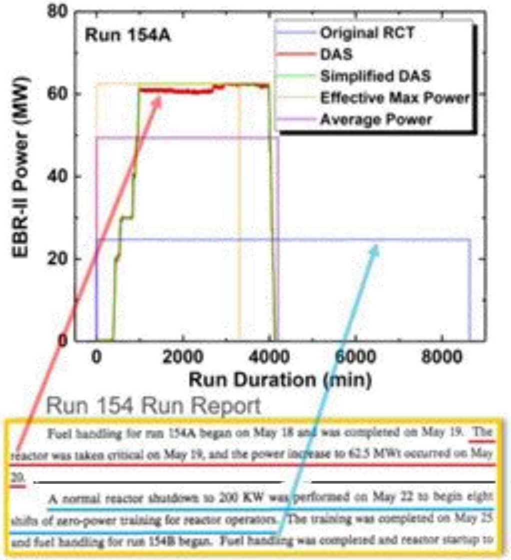

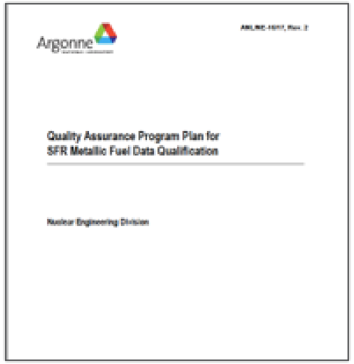

FIPD QA Being Performed Following NRC Approved QAPP

†FIPD (Metallic Fuels Irradiation & Physics Database) is supported by US DOE-NE's Advanced Reactor Technologies (ART) Fast Reactor Program (FRP) and NE-4 Advanced Fuels Campaign (AFC).

U.S. DEPARTMENT of ENERGY | Office of Nuclear Energy

BISON-OPTD Integration

- Assessment Using OPTD† Database
  - Out-of-pile Transient Experiments
    - Fill gap between TREAT (M-series) & EBR-II tests
      - Models can be used by them in the future
    - FBTA and WPF (FM-series)
  - Use BISON-FIPD for steady-state
    - Initial conditions for out-of-pile transient cases
  - Use BISON-OPTD for transient
    - Implement models to cover all essential physics
    - Create assessment case for V&V
      - 4 FBTA tests & WPF-1

Steady-State Irradiation (FIPD-BISON) T437/X425 — **Solution Data** disp, porosity, …
→ **Out-of-Pile Experiment (OPTD-BISON)** FBTA 88-04 — **New Mesh** Restart with SS solution data

Steady-State Irradiation (FIPD-BISON) T418/X425 — **Checkpoint Data** All recoverable data
→ **Out-of-Pile Experiment (OPTD-BISON)** FM-1 — **Same mesh** Restart with checkpoint

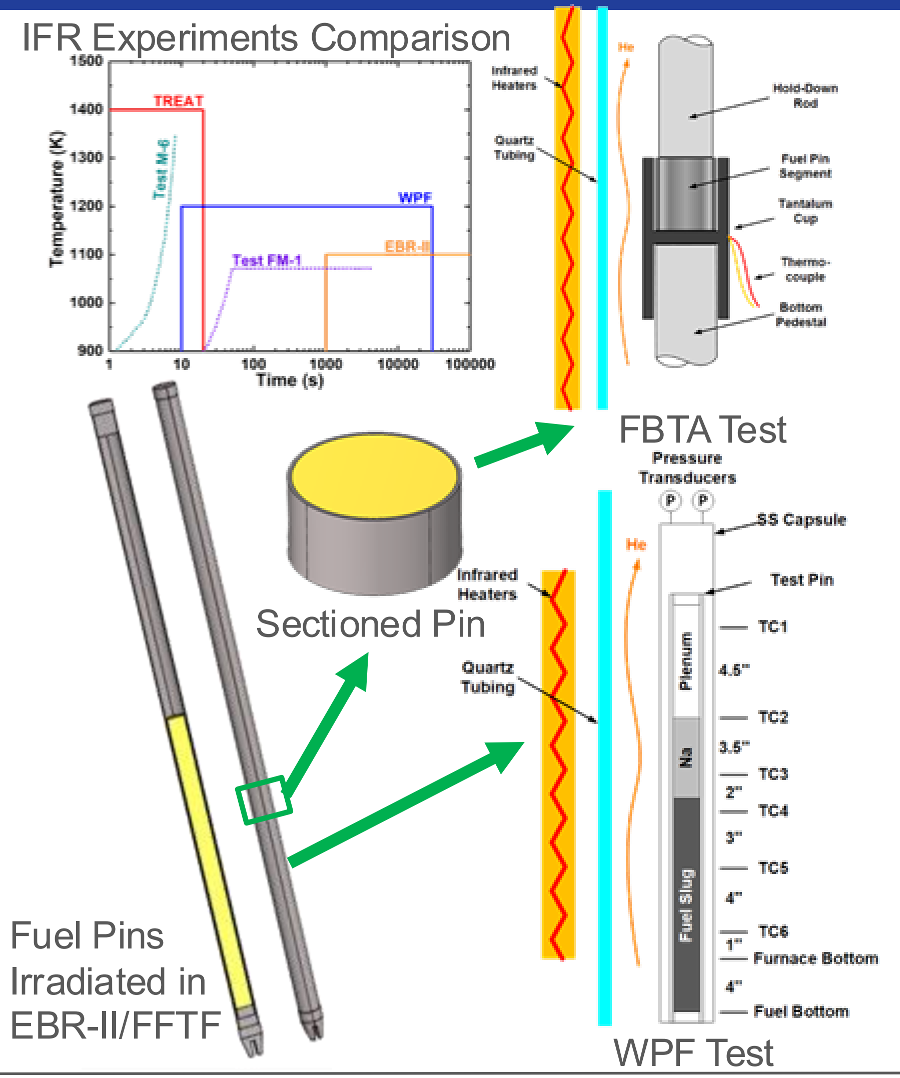

†OPTD (Out-of-Pile Transient Database) is supported by US DOE-NE's Advanced Reactor Technologies (ART) Fast Reactor Program (FRP).

Databases Integration Framework

- FIPD Integration Objects in BISON
  - Mesh Generation
  - Irradiation Conditions
  - PIE Comparisons
- Data Integration
  - Data Submodule of BISON
    - FIPD
      - Pin design parameters
      - Operating conditions
      - NRAD/profilometry,…
    - OPTD
      - Pin information
      - Furnace test conditions
      - Penetration/liquefaction

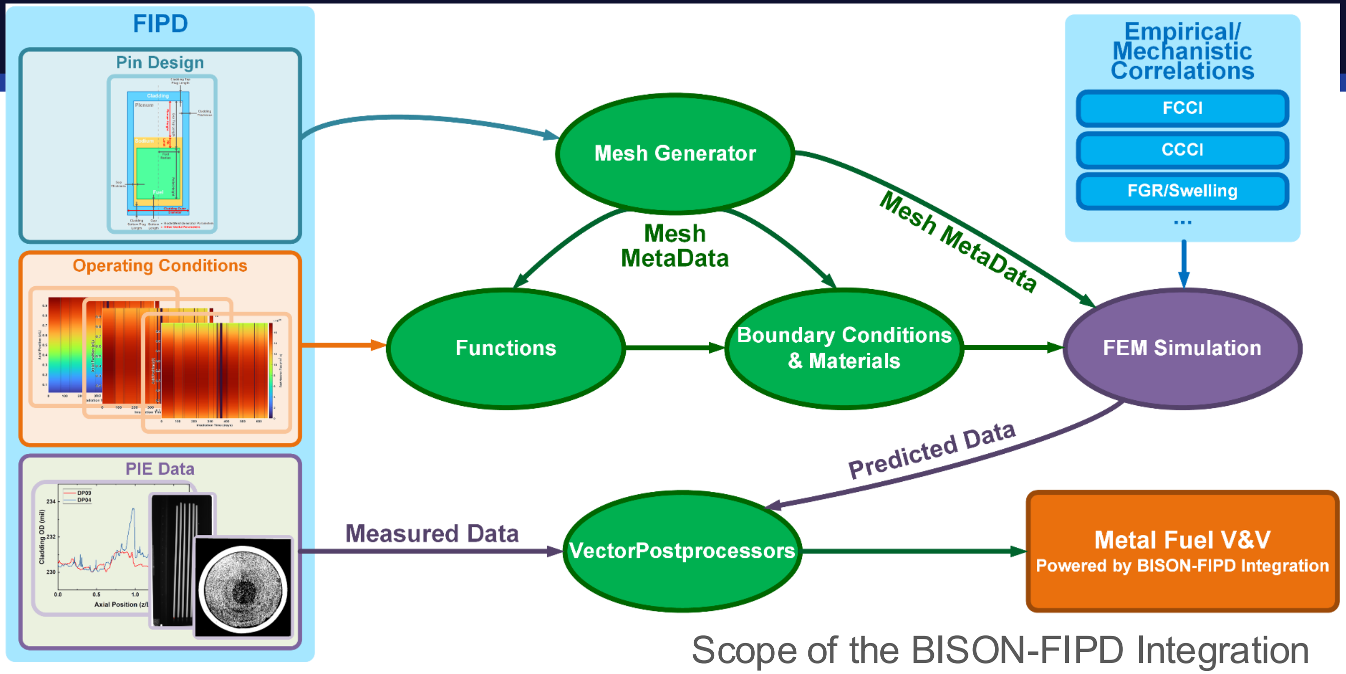

Scope of the BISON-FIPD Integration

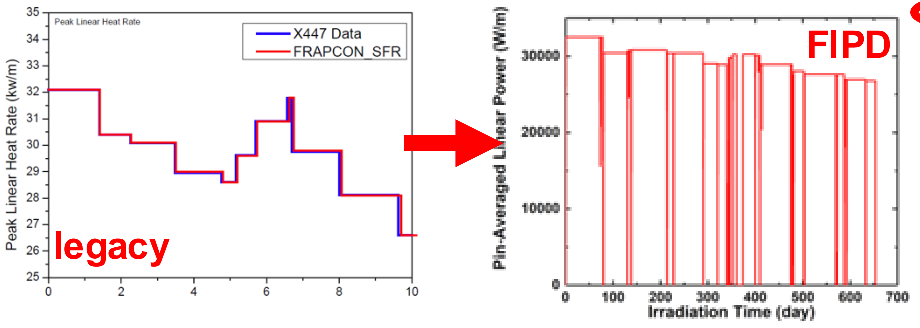

Detailed Operating Conditions from FIPD

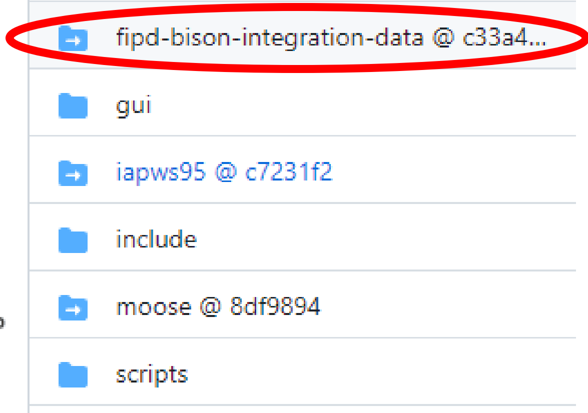

Data Submodule in BISON

Overview: Databases Powered Validation Platforms

- Assessment cases powered by FIPD/OPTD integration
  - Steady State / Normal Operation
    - (EBR-II) X447 → High temperature fuel-cladding compatibility (FCCI) – **FY24 Enhancements**
    - (EBR-II) X423 → Low burnup fuel swelling behavior / "Fat" fuel slugs
    - **(EBR-II) X425 → High burnup cladding behavior (FCMI)**
    - **(EBR-II) X441 → enhance existing important X441 assessment case**
    - **(EBR-II) X501 → TRU-loaded fuel**
      - **Potential (Phenix) METAPHIX-Series**
  - Out-of-Pile/Furnace Transient
    - **(FBTA) 124 Tests → cladding-fuel interface liquefaction in irradiated fuel**
    - (WPF) FM-1 → short-term cladding failure at over temperature
      - **More FM-Series tests with a focus on long-term demonstration tests**

- Prior FYs
- **FY24 Achievements**
- **FY25 Ongoing**
- **Planned**

X447 Assessment Case

[1] Y Miao et al., *Nucl. Eng. Des.*, 385 (2021) 111531
[2] https://mooseframework.inl.gov/bison/metallic_fuel/EBRII/X447/doc/X447.html
[3] https://mooseframework.inl.gov/virtual_test_bed/sfr/ebr2_x447_dp11/index.html
[4] L Aagesen et al., INL/RPT-24-81050 (2024)

- Cladding Degradation Model Evaluation
  - Integral Fast Reactor Program X447 Experiment
    - **<u>U-10Zr/HT9:</u>** 15 pins to 10 at.%; 8 pins to 5 at.%
    - Hi-Temp (>600°C) FCCI found to limit the fuel operating envelope
    - 2 of 15 U-10Zr/HT9 pins irradiated to ~10% BU failed
  - Up-to-date modeling approaches including Mortar and AD
  - Demonstration of BISON-FIPD Integration
    - More consistent prediction using FIPD-based data
    - VTB Demonstration Example (DP11)

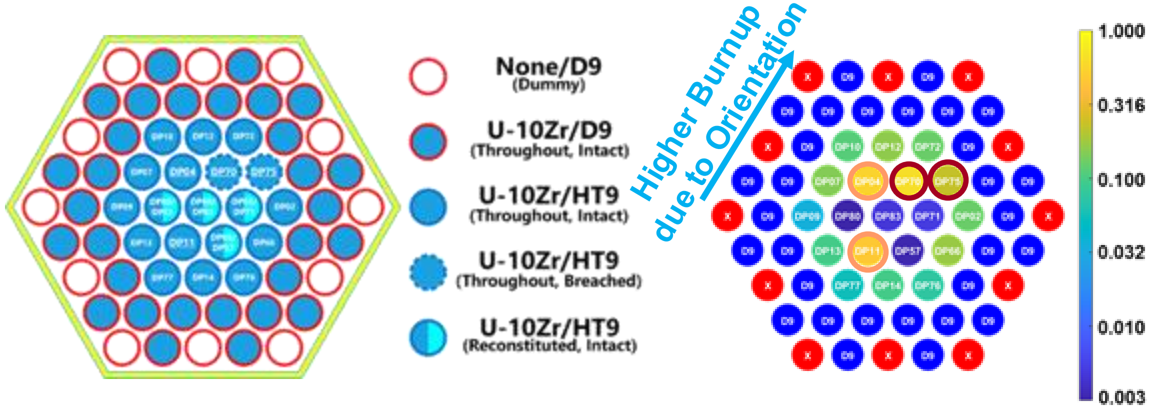

X447/A Subassembly and CDF predicted for HT9 pins [1]

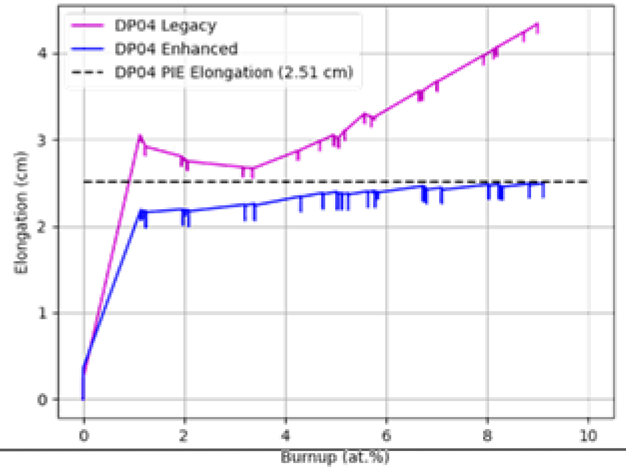

Predicted fuel elongation compared with PIE (DP04).

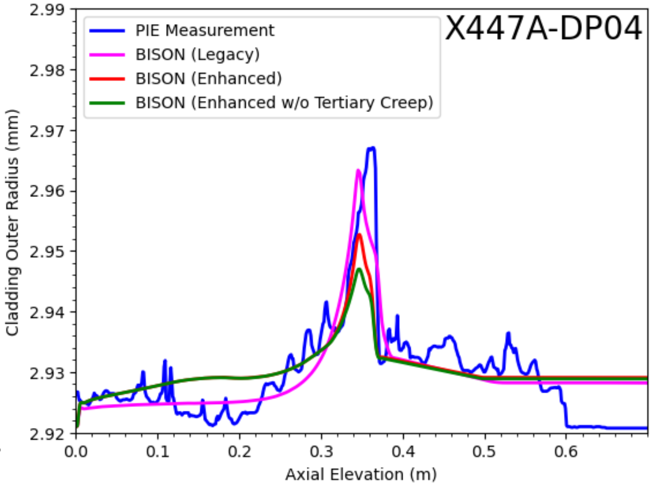

Predicted cladding deformation compared with PIE (DP04).

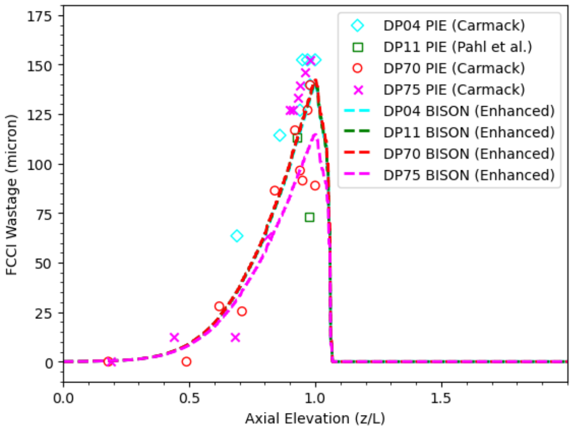

FCCI Wastage: BISON vs. PIE

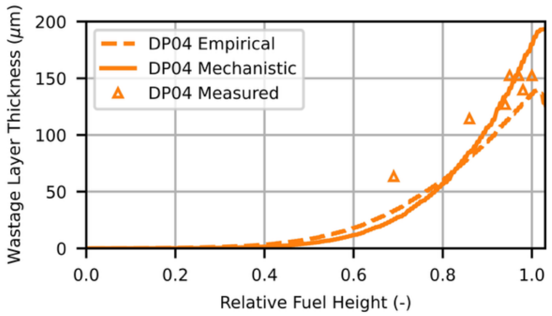

Mechanistic FCCI model validation using the assessment case [4]

[1] A.M. Yacout et al., ANL-IFR-172

X425 Assessment Case (FY25 Ongoing)

- High-Burnup Behavior (FCMI) Assessment
  - Integral Fast Reactor Program X425 Experiment
    - **U-10Zr-xPu fuel** + HT9 Cladding
      - 17 U-10Zr pins; 11 U-8Pu-10Zr pins; 2 U-19Pu-10Zr pins
      - Reach ~20 at.% burnup
    - Three reconstitution for PIEs
      - Profilometry at ~3 at.%, 10 at.%, 16 at.% and 20 at.% burnup
  - Two main focuses
    - FCMI and cladding deformation
      - Mortar contact model/friction coefficient
      - Fuel hot pressing/cladding creep models (MFH/surrogate models)
    - Fuel axial growth
      - Anisotropy: Pu dependence and difference for “fat” slugs (X423 and X430)
      - Mortar contact model/friction coefficient

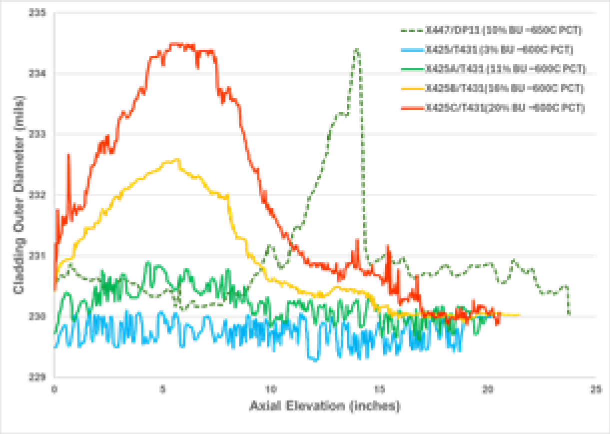

Comparison b/t FCMI (X425) and FCCI (X447) dominated cladding deformation

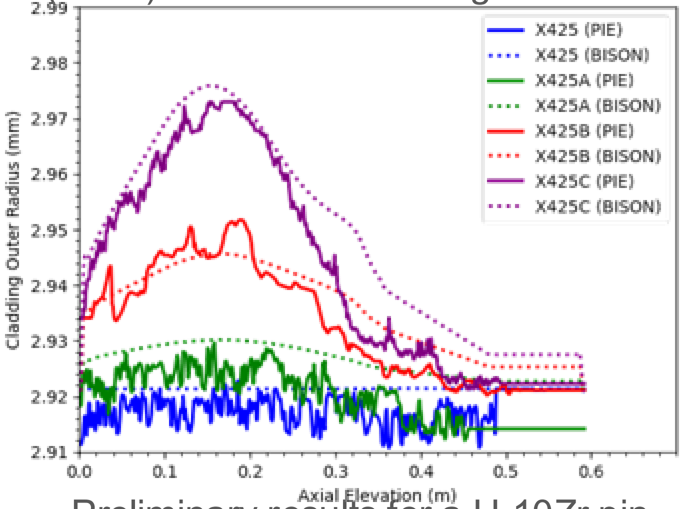

Preliminary results for a U-10Zr pin

TRU Irradiation Experiments (Planned)

[1] M.K. Meyer et al., *J. Nucl. Mater.*, 392 (2008) 176
[2] L. Capriotti et al., *J. Nucl. Mater.*, 539 (2020) 152279
[3] H. Ohta et al., *Nucl. Technol.*, 190 (2015) 36

- TRU-Involved Experiments
  - IFR Experiment X501
    - 2 irradiated pins
      - U-20.2Pu-9.1Zr-1.2Am-1.3Np
      - ~7 at.% burnup
    - FIPD-BISON integration
  - METAPHIX-Series Experiments
    - 3 irradiated pins per capsule
      - U-19Pu-10Zr
      - U-19Pu-10Zr-2MA-2RE/5MA-5RE/5MA
      - 3 capsules → 2.5, 7, and 10 at. % burnup
    - BISON simulations (IAEA benchmark)
      - METAPHIX-1 and METAPHIX-2

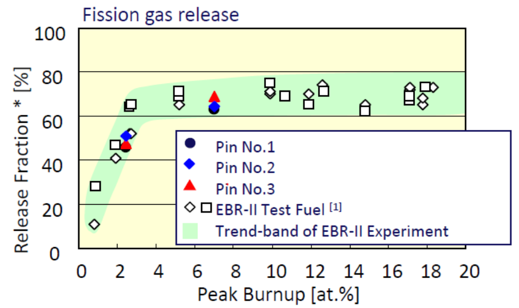

Similar FGR behavior

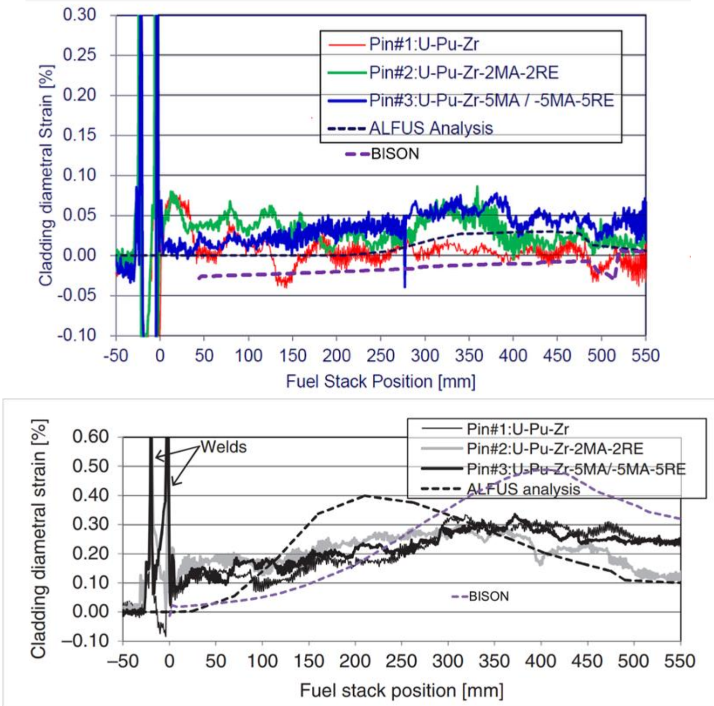

METAPHIX Cladding Deformation
(ALFUS data, courtesy of T. Ogata)

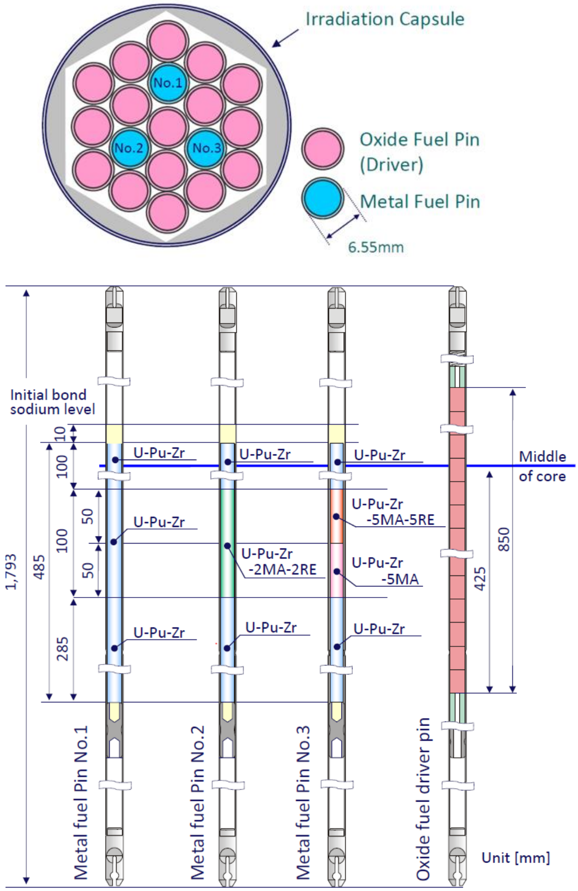

METAPHIX Series Experiments

FBTA Assessment Case

[1] Y Miao et al., *ANL/NEAMS-23/6*, 2023
[2] https://mooseframework.inl.gov/bison/metallic_fuel/FBTA/doc/FBTA.html

- FBTA Tests Coverage
  - (Baseline) 4 tests based on X425/T437
  - (Comprehensive) 124 tests based on 23 irradiated pins
- Fuel-Cladding Interface Liquefaction
  - Legacy Tsai + updated ANL correlations for cladding
  - Improved fuel liquefaction correlation
- Impacts of the Assessment Case
  - Eutectic cladding penetration model V&V
  - Platform for statistic studies

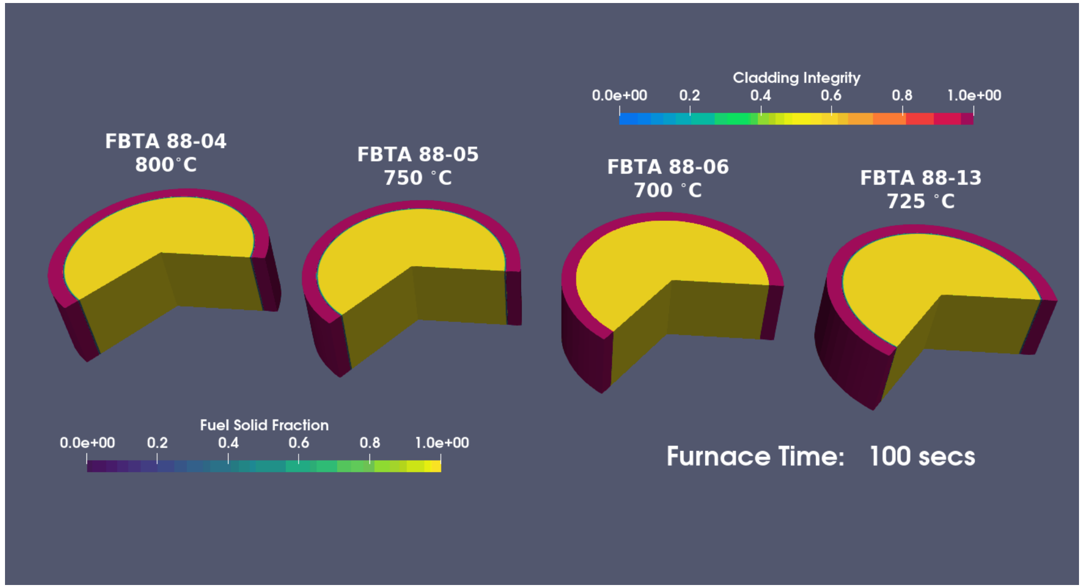

BISON prediction using Tsai-Bauer Correlation

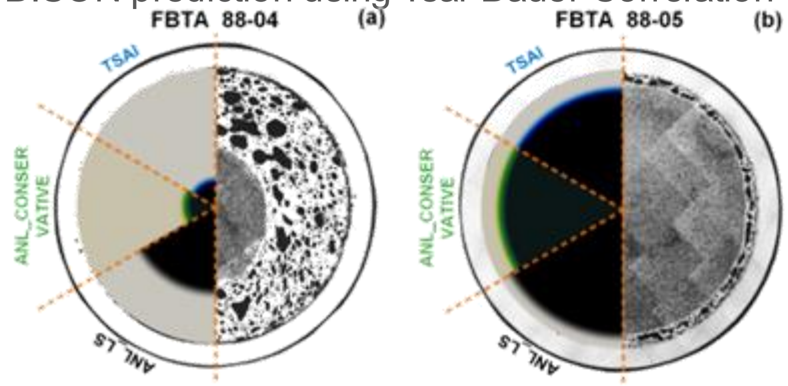

Post-FBTA metallographs of the four tested sections

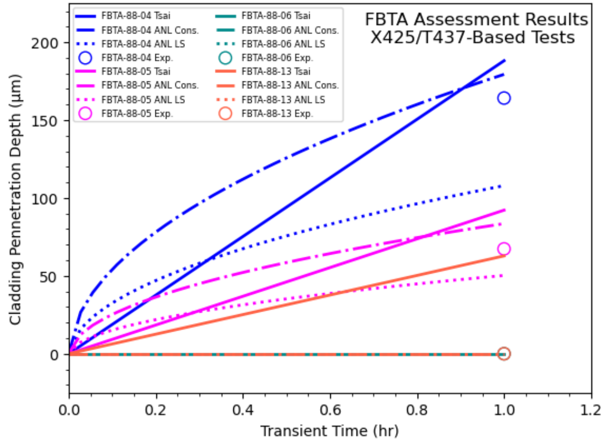

Cladding Penetration Comparison
(four tests based on T437)

FBTA Assessment Case

[1] Y Miao et al., *ANL/NEAMS-24/1*, 2024
[2] https://mooseframework.inl.gov/bison/metallic_fuel/FBTA/doc/FBTA.html

- Full FBTA coverage
  - 23 irradiated pins → 124 FBTA tests
  - Binary + 5 Pu contents
  - HT9, CWD9, CW316SS
- Comprehensive validation platform
  - Empirical models
  - Mechanistic and AI/ML models

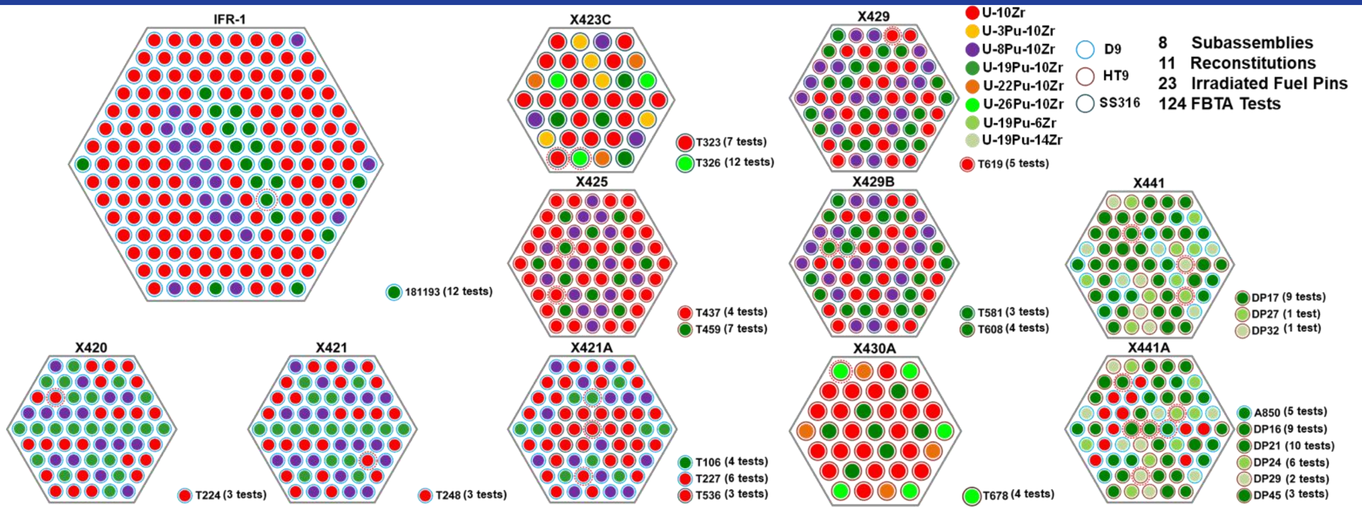

Summary of covered FBTA tests and used irradiated pins

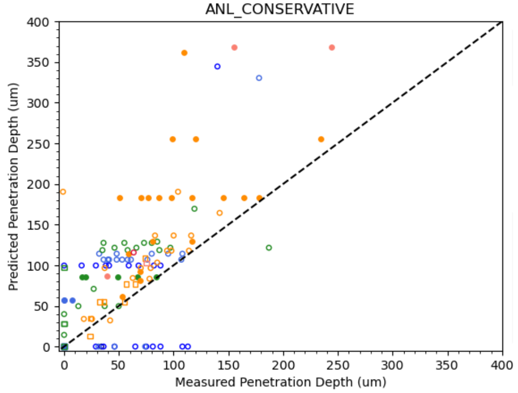

ANL conservative cladding penetration model

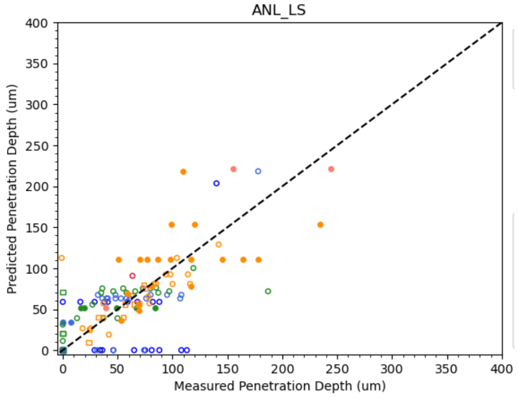

ANL best fitting cladding penetration model

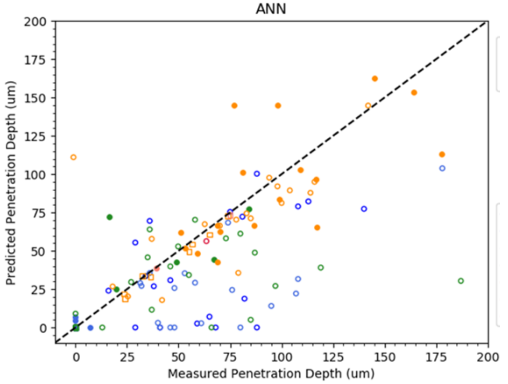

Demo of a preliminary artificial neural network surrogate model (MOOSE-libTorch)

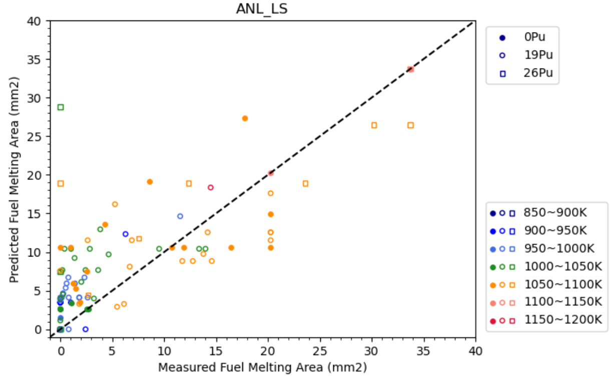

ANL best fitting cladding penetration model in fuel liquefaction prediction

Conclusions

- Databases-Powered Validation Achievements Highlight
  - Established BISON-FIPD and BISON-OPTD integration for metallic fuel models validation.
  - Steady-state
    - X447: FCCI & cladding degradation at high temperatures (milestone report, assessment, paper, VTB)
    - X423: fuel volumetric swelling (milestone report, assessment, paper)
    - X425: fuel-cladding mechanical interaction (assessment in preparation)
  - Transient performance
    - FBTA: systematic fuel-cladding liquefaction (milestone report , assessment, paper in preparation)
    - WPF FM-1: run-to-breach furnace test (milestone report, assessment)
- Future Work
  - Expand the coverage of the databases-powered validation platforms
  - Investigate an extensive set of mechanistic models using such platforms
  - Go beyond the current axisymmetric single-pin scheme to support assembly level assessment

An overview of mechanistic cladding-side FCCI model development and preliminary validation

Jacob Hirschhorn, Larry Aagesen, Chao Jiang, and Boone Beausoleil

Cladding-side FCCI background

- Lanthanide fission products migrate to the cladding to form brittle intermetallic phases, which are considered strengthless wastage
- Experimental observations have correlated the axial distributions of radial cladding deformation, lanthanide activity, power density, and temperature, hinting at the impacts of lanthanide production and transport
- Other observations have linked FCCI to fuel cracking
- Observations hint at transport mechanisms and the roles of various microstructural features

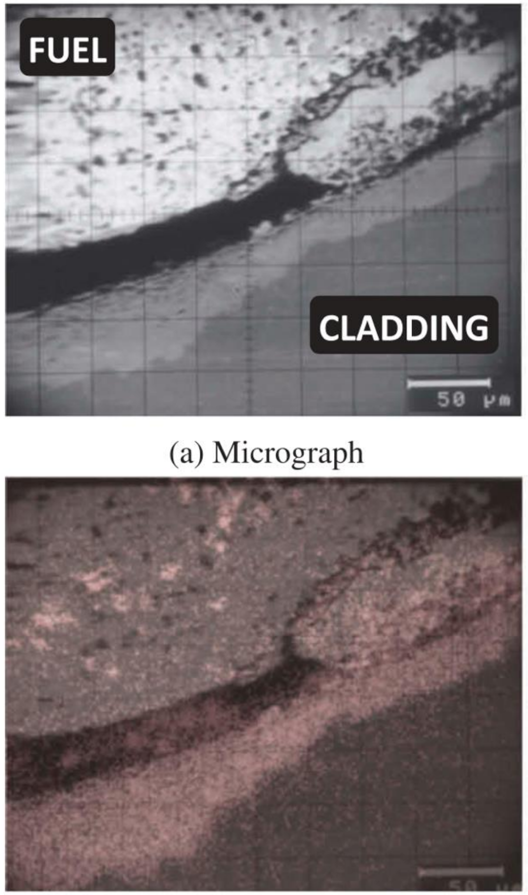

(a) Micrograph

(d) Neodymium overlaid on micrograph

Cladding-side FCCI framework:

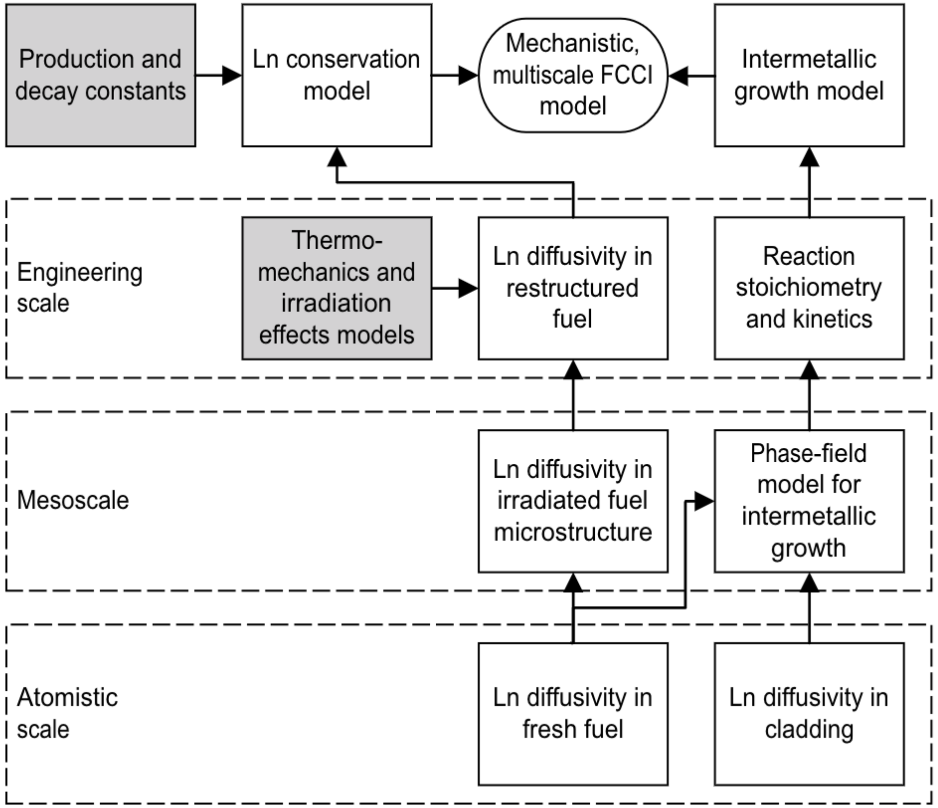

C. Matthews, et al., Nuclear Technology 198:3 (2017) 231–259.
J. Hirschhorn, et al., Nuclear Engineering and Design 432 (2025) 113811.

Atomistic parameters are weighted in mesoscale simulations

- Lanthanide transport in the fuel is described by a temperature- and microstructure-dependent diffusivity, which accounts for
  - Solid-state diffusion
  - Liquid-like transport associated with porosity development, porosity interconnection, and sodium infiltration

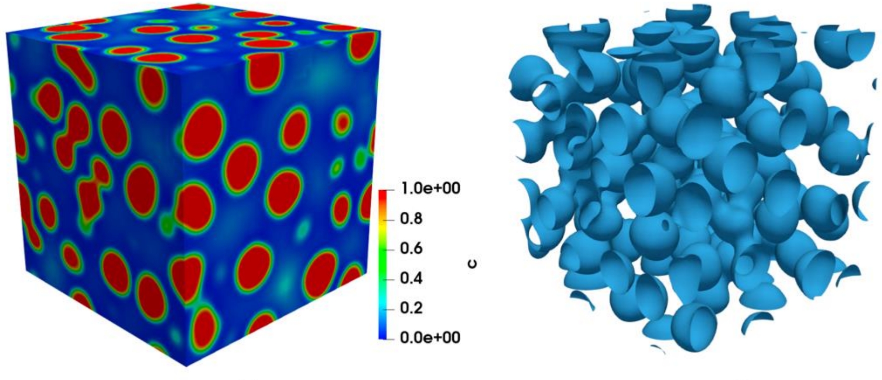

(a) (b)

- These features account for temperature and energy deposition (through dependence on microstructure)

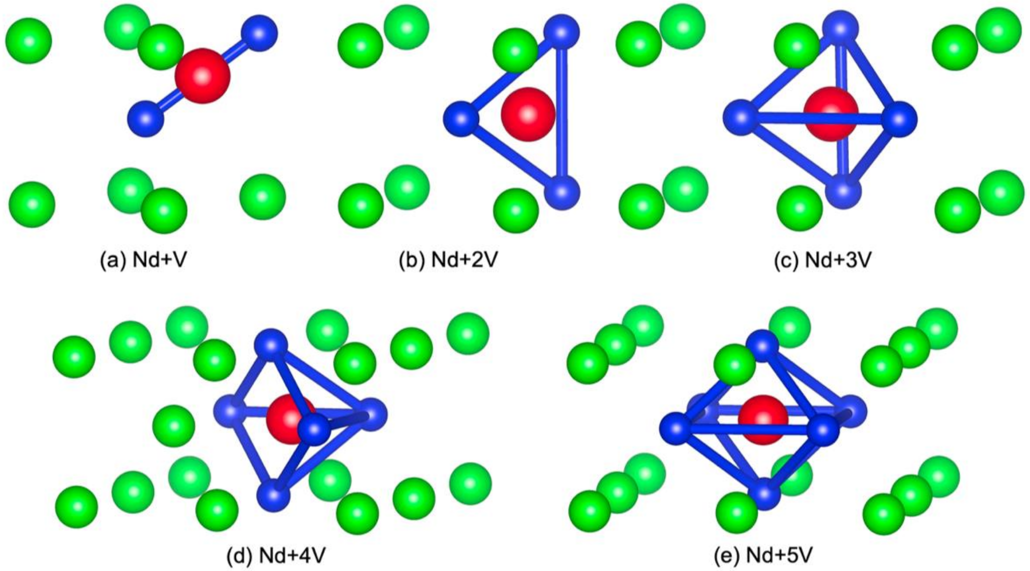

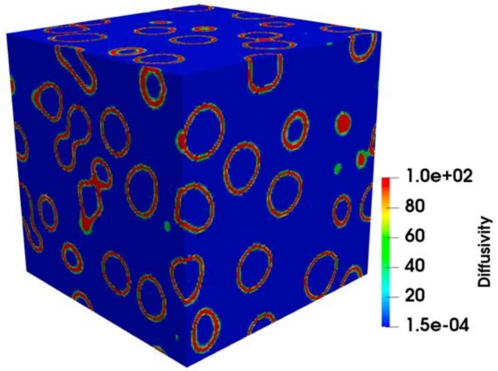

(c)

L. Aagesen, et al., INL/RPT-23-74500.

Preliminary model demonstration and validation

- A 1D phase-field model of the fuel-intermetallic-cladding was developed to study growth kinetics
- The engineering scale model considers
  - Lanthanide conservation in the fuel using a source term from the literature
  - Reaction using a boundary condition on the fuel surface
- Predicted wastage can be coupled back into the cladding mechanics solve by modifying the cladding stress or elastic properties
- Multiscale coupling was used to guide engineering scale development
- Simulations used EBR-II experiment X447 fuel rod DP75
- Optimization was used to account for uncertainties related to which process(es) limit wastage formation, e.g., reactant availability (fission source and fuel transport), fuel cracking and potential Zr rind disruption, reactant transport through the gap, and reactant transport through the reaction layer and the rate of reaction

Lanthanide conservation
$$\frac{\partial c}{\partial t} = \nabla \cdot D\nabla c + \dot{F}\gamma - \lambda c,$$

Reaction boundary condition
$$J = -D\nabla c = M_0 \exp\left(\frac{-E_a}{kT}\right)\left(c - c_{eq}\right),$$

Wastage velocity
$$v = f_S V_m f_G f_{TV} J,$$

Geometry factor
$$f_G = \frac{R_f}{R_f + t_g + \delta},$$

Azimuthal heterogeneity
$$f_{TV} = \frac{\delta_{max}}{\delta_{uniform}},$$

Incremental growth
$$\delta = \sum_{i=1}^{I} \delta_{i-1} + v_i \Delta t_i.$$

J. Hirschhorn, et al., Nuclear Engineering and Design 432 (2025) 113811.

Multiscale coupling and optimization using fuel rod DP75

- Wastage thickness was measured at 10 heights
- Existing engineering scale BISON assessments provided realistic irradiation conditions and microstructural evolution, i.e., fission rate density, temperature, porosity, and pore sodium content
- Local phase-field intermetallic growth simulations predicted resulting layer velocities
- Flux boundary condition parameters were optimized to match observed wastage profiles

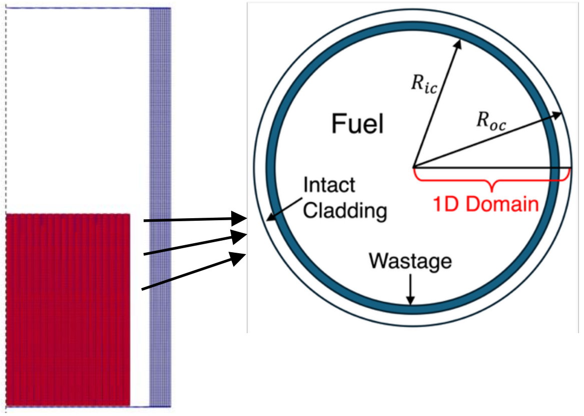

EBR-II X447 DP75
(radius × 100)

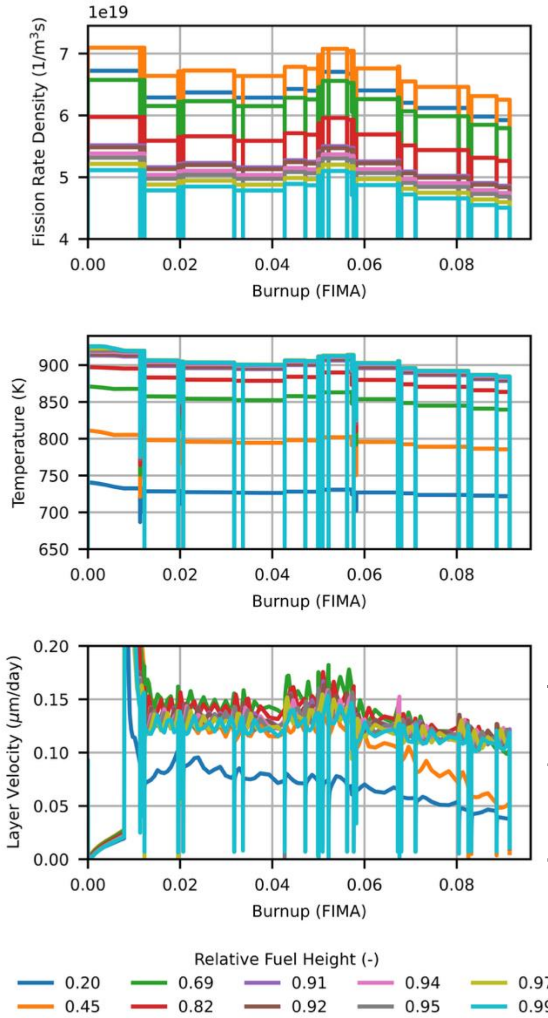

Approximately linear growth

$$J = -D\nabla c = M_0 \exp\left(\frac{-E_a}{kT}\right)(c - c_{eq}),$$

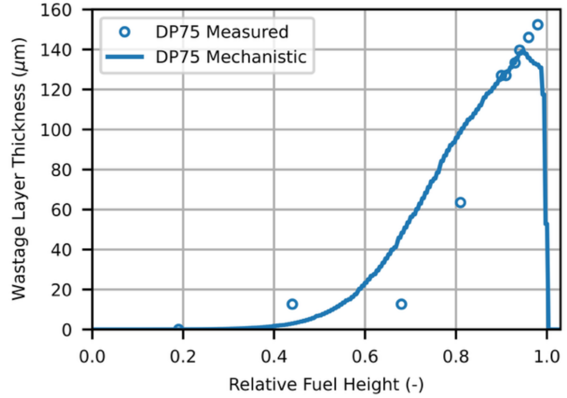

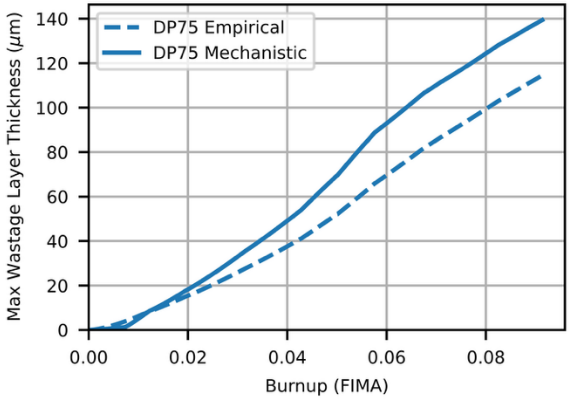

J. Hirschhorn, et al., Nuclear Engineering and Design 432 (2025) 113811.

Preliminary model demonstration and validation

- The optimized model was validated against radial cladding dilation and wastage thickness measurements from 3 additional fuel rods from EBR-II experiment X447
- It was then applied to predict wastage for a commercial-length fuel rod from FFTF experiment IFR1, where it predicted the expected magnitude of peak wastage and the shift in its axial position toward the fuel midplane, potentially due to the impacts of varying fission rate density and temperature (and the spatial distributions thereof)

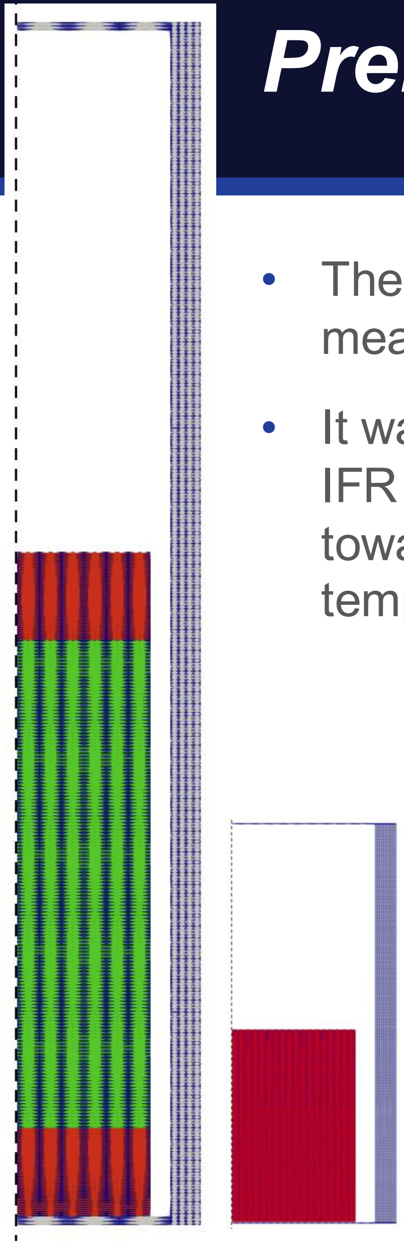

FFTF IFR1 fuel rod (left)
EBR-II X447 fuel rod (right)
(radius × 100)

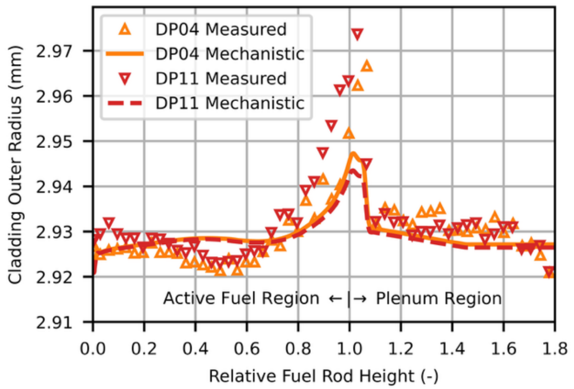

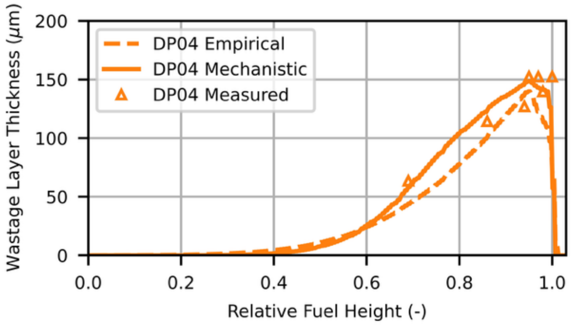

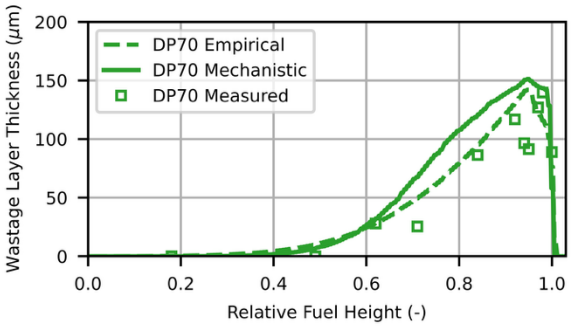

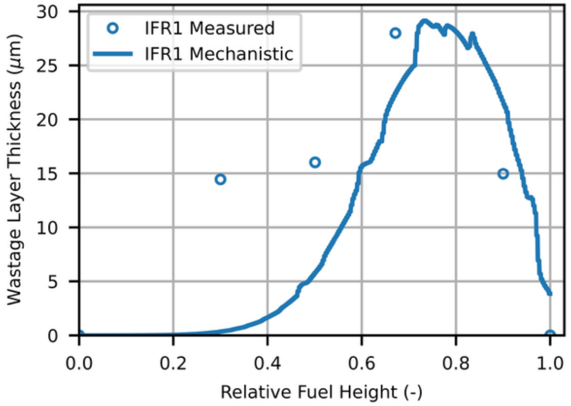

J. Hirschhorn, et al., Nuclear Engineering and Design 432 (2025) 113811.

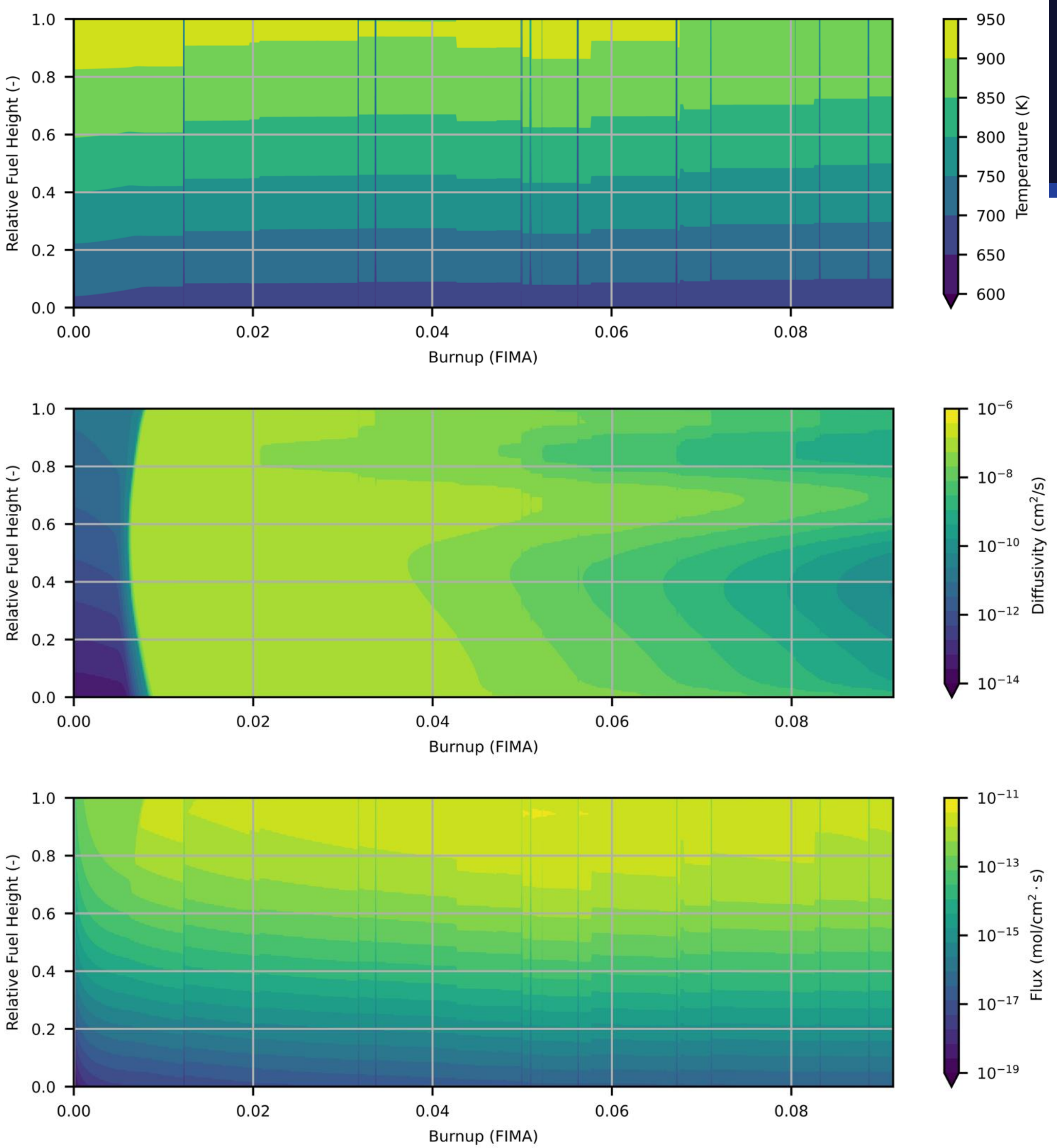

A closer look at DP75

- The spatial and temporal temperature surface reveals the high fidelity of operating conditions sourced from the Metallic Fuel Irradiation & Physics Database
- The diffusivity surface illustrates changes in lanthanide transport due to solid state diffusion; porosity development, interconnection, and sodium infiltration; and porosity collapse due to hot pressing
- The flux surface illustrates how lanthanides might behave in the fuel to produce the observed wastage behaviors
- This modular framework yields observables that can be compared to experiments

J. Hirschhorn, et al., Nuclear Engineering and Design 432 (2025) 113811.

NEAMS Outlook: Metallic fuel

Summary

- Baseline capabilities in place
- V&V through BISON-FIPD/OPTD integration
  - Maintenance and enhancement of X447 Assessment Case
  - Establishment of X423/X425 Case
  - Improvement of liquid phase penetration models
- New mechanistic FCCI model ready for use
- Continued assessment support

Next Steps

- Prioritized tasks by stake-holder interest:
  - Improvement of hot-pressing model using mechanistically sound models?
  - Implementation of new HT9 LaRomance models as available (coupled with FCCI)?
  - Resurrect fast running 1.5D simulations?
  - Incorporation of minor actinides?
  - Transient fuel modeling?

Overall status for metallic fuel: Good progress we can stand on

Need to: 1) grow assessments based on FIPD,

2) start executing the next challenge problem

U.S. DEPARTMENT of ENERGY

Office of Nuclear Energy